

Warming of the Willamette River, 1850–present:

~~†The effects of climate, change and watershed flow management river system alterations change and direct human interventions~~

Formatted: Strikethrough

S.A.Talke¹, D.A.Jay², H.L. Diefenderfer^{3,4}

¹Civil and Environmental Engineering, California Polytechnic State University, San Luis Obispo, California

²Civil and Environmental Engineering, Portland State University, Portland, Oregon

³Coastal Sciences Division, Pacific Northwest National Laboratory, Sequim, Washington

⁴School of Environmental and Forest Sciences, University of Washington, Seattle, Washington

Correspondence to: Stefan A. Talke (stalke@calpoly.edu)

Keywords: ~~Water Temperature~~Water Temperature, Climate Change, River regulation, Anthropogenic Effects

Key Points

- A statistical model based on archival records ~~back to~~from the 1850s onwards shows that average ~~water temperature~~ water temperature has increased by 1.1 °C/century since the mid-19th century
- Water temperature is less variable than historically, and the deeper modern river system is less influenced by extreme heat waves or cold weather anomalies.
- Warming air temperatures are the most important factor in modeled increases in water temperature, with river system changes most influential during the cool season. The largest increases in water temperatures water temperature occur in January–February (–1.3 °C/century), and while the smallest are in May–June (–0.8 °C/century)
- The number of warm water days (above 20 °C) has increased by 3 weeks, matched by a similar decrease in the number of days below 4 °C
- Approximately 30% of the increased water temperature water temperature is attributable to system changes flow management, and 70% to warming air temperature (climate change)

Abstract

Using archival research methods, we ~~found-recovered~~ and combined data from multiple sources to produce a unique, 140-year record of daily ~~water temperature~~~~water temperature~~ (T_w) in the lower Willamette River, Oregon (1881–1890, 1941–present). Additional daily weather and river flow records from the 1850s onwards are used to develop and validate a statistical regression model of T_w for 1850–2020. The model simulates the time-lagged response of T_w to air temperature and river flow, and is calibrated for three distinct time periods: the late 19th, mid 20th, and early 21st centuries. Results show that T_w has trended upwards at ~ 1.1 °C /century since the mid-19th century, with the largest shift in January/February (1.3 °C /century) and the smallest in May/June (~ 0.8 °C /century). The duration that the river exceeds the ecologically important threshold of 20 °C has increased by ~~about~~ 20 days since the 1800s, to ~~about~~ 60 d yr⁻¹. Moreover, cold water days below 2 °C have virtually disappeared, and the river no longer freezes. Since ~ 1900 , changes are primarily correlated with increases in air temperature (T_a increase of 0.81 ± 0.25 °C) but also occur due to ~~increased reservoir capacity, altered land use and river morphology, and other anthropogenic changes~~ alterations in the river system such as depth increases from reservoirs (0.34 ± 0.12 °C). Managed release of water influences T_w seasonally, with an average reduction of ~~0.27 °C and up to~~ 0.56 °C estimated for ~~August and~~ September. River system changes have decreased daily variability (σ) by 0.44 °C, increased thermal memory, ~~and reduced interannual variability, and reduced the response to short-term meteorological forcing (e.g., heat waves)~~. These system changes fundamentally alter the response of T_w to climate change, posing additional stressors on fauna.

Short Summary

We use archival measurements and a statistical model to show that average water temperature in a major US West Coast river has increased by 1.8 °C since 1850, at a rate of 1.1 °C /century. The largest factor driving modeled changes are warming air temperatures (nearly 75%). The remainder is primarily caused by depth increases and other modifications to the river system. Near-freezing conditions, common historically, no longer occur, and the number of warm water days has significantly increased.

~~This manuscript uses archival measurements and a statistical model to show that water temperaturewater temperatures in the Willamette River have trended upwards since 1850, with the largest increase occurrences in winter and the smallest (~ 0.8 °C /century) in late spring. Approximately 30% of the increase is attributable to changes in watershed system changes, and 70% to warming air temperature (climate change). The number of warm water days has significantly increased, and near-freezing conditions, common historically, no longer occur.~~

1.0 Introduction

~~Water temperature~~Water temperatures are rising in many temperate streams and rivers, in part due to climate change, (e.g., Kaushal et al., 2010). Beyond a warming climate, many additional factors influence water temperature (T_w), including land-use patterns and development, deforestation, water withdrawal and return flows, reservoir storage, and other types of water-resources

70 management (e.g., [Kaushal et al., 2010](#); [Olden & Naiman, 2010](#); [Bottom et al., 2011](#)). [Assessing long-term temperature trajectories and understanding their causes is vital, b](#)
 71 [Because wa-](#)
 72 [ter temperaturewater temperature \(\$T_w\$ \) influences ecological processes, water quality, oxygen](#)
 73 [levels, and fish habitat and survivability \(e.g., \[Caissie, 2006\]\(#\); \[Bottom et al., 2011\]\(#\); \[Clemens\]\(#\)](#)
 74 [2022\).](#), [defining long-term temperature trends and understanding their causes is vital.](#) However,
 75 with few exceptions (e.g., [Webb & Noblis, 2007](#); [Pohle et al., 2019](#)), few T_w records from the late
 76 19th or early 20th century have been [recovered or](#) evaluated, particularly in North America
 77 ([Kaushal et al., 2010](#)). [Historical, pre-development baselines are therefore difficult to assess, be-](#)
 78 [cause many \(often most\) watershed changes, like reservoir construction, precede the start of](#)
 79 [available thetemperature records \(e.g., \[reservoir construction\]\(#\)\).](#) Additionally, interannual and de-
 80 cadal variability in climate can mask or bias trends in short records (e.g., [El Nino/La Nina or the](#)
 81 [Pacific Decadal Oscillation; see \[Peterson & Kitchel, 2001\]\(#\); tropicalization see \[NASEM 2022\]\(#\),](#)
 82 [Greening et al. 2022\).](#) The limited availability of earlier records inhibits the ability to discern
 83 secular trends, evaluate causes, and assess impact. There is, therefore, a need to digitizeIn this
 84 study, we find, recover and analyze previously forgotten or unused archival T_w water temperature
 85 recordsrecords from [as early as the late 19th century1881 forwardonward fromfor the lower](#)
 86 [Willamette River. These records, which precede most industrialization and modern development](#)
 87 [in the Pacific Northwest, enableprovide a unique,](#) such as those collected daily by the US Signal
 88 Service in the 1880s at 20+ coastal and river stations (see the Monthly Weather Review series of
 89 publications, volume 9 to 18)- opportunity to discern secular trends, evaluate and attribute
 90 causes, and assess the net impact of human activities in a temperate coastal river.

Formatted: Superscript

91
 92 [The changes to the Willamette River watershed over the past 150 years are substantial and mirror](#)
 93 [other regions. Like many other rivers worldwide \(e.g., \[Piegay et al. 2000\]\(#\); \[Ralston et al., 2019\]\(#\)\),](#)
 94 [the Willamette River is more channelized, deeper, and reduced in length compared to 19th cen-](#)
 95 [tury conditions \(e.g., \[Piegay et al. 2000\]\(#\); \[Ralston et al., 2019\]\(#\); \[Sedell & Froggatt, 1984\]\(#\); \[Benner &\]\(#\)](#)
 96 [Sedell, 1997; \[Gregory et al., 2002a\]\(#\)\).](#) [The migration and spawning of Willamette River fish such](#)
 97 [as Pacific lamprey \(*Entosphenus tridentatus*\) \(\[Clemens et al. 2022\]\(#\)\) and Chinook, coho, and](#)
 98 [chum salmon \(\[Richter and Kolmes 2005\]\(#\)\) are directly impacted by these temperatures in the](#)
 99 [Willamette \(\[Clemens et al. 2022\]\(#\)\).](#) Similar to other temperate-zone rivers ([Knowles & Cayan,](#)
 100 [2002, \[Cloern et al., 2011\]\(#\), \[Stewart et al., 2005\]\(#\), \[Webb & Noblis, 2007\]\(#\)\), the seasonal flow regime](#)
 101 [has been altered by reduced snow-pack and by the construction of flood-control and storage res-](#)
 102 [ervoirs \(\[Payne, 2002\]\(#\), \[Rounds, 2010\]\(#\)\). Beginning in the 19th century, logging within the water-](#)
 103 [shed and deforestation of the riparian corridor decreased shading \(\[Gregory et al. 1991\]\(#\), \[Johnson\]\(#\)](#)
 104 [& \[Jones, 2000\]\(#\), \[Wallick et al. 2022\]\(#\)\).](#)- Urbanization, water diversions, effluent discharges, hydro-
 105 electric projects, and storage for agriculture have also likely shifted T_w ([Berger et al., 2004](#), [OR](#)
 106 [DEQ, 2006](#)). Such processes have influenced T_w water temperature in many other regions (e.g.,
 107 [Nelson and Palmer, 2007; \[Kinouchi et al., 2007\]\(#\); \[Palmer et al., 2010\]\(#\)](#)). Because of a lack of in-situ
 108 data from pre-reservoir conditions, the cumulative effect of anthropogenic influence is currently
 109 unknown ([OR DEQ, 2006](#)).- Here, we analyze the net effect of anthropogenic stressors by devel-
 110 oping statistical models from in-situ data that {approximately} represent pre-development condi-
 111 tions (pre-1890);- post-land and river development conditions (mid 20th century); and post-reser-
 112 voir management conditions (present-day).

Formatted: Not Highlight

Formatted: Not Highlight

Formatted: Not Highlight

Formatted: Highlight

Formatted: Font: Italic

Formatted: Not Highlight

In the Pacific Northwest, T_w controls the long-term viability of salmon and other endangered species (Mantua, 2010; Bottom et al., 2011; Isaak et al., 2012; Caldwell et al., 2013). Above a threshold of 18–21 °C, various species of salmon, steelhead, and trout are stressed and become more susceptible to disease (OR DEQ, 2006; Mantua, 2010). As a result, regulations require that the seven-day average of the daily maximum temperature should not exceed 20 °C, with a lower threshold set for rearing and spawning streams (e.g., OR DEQ, 2006). An allowance of 0.3 °C is permitted for the sum of all anthropogenic point sources such as wastewater discharge, and non-point sources such as loss of shading or heating in reservoirs. Hence, the Willamette River in Portland, Oregon (Figure 1) is considered an impaired water body and out of regulatory compliance for T_w above 20.3 °C (OR DEQ, 2006).

Accurately assessing and disentangling anthropogenic and climate change influences is challenging because of the large number of alterations and anthropogenic uses (e.g., diversions and discharges), and feedbacks between different factors. Compared to its natural state, the Willamette River is more channelized, deeper, and reduced in length (particularly in upstream reaches; e.g., Sedell and Froggatt, 1984; Benner and Sedell, 1997; Gregory et al., 2002a). The construction of large storage reservoirs (Payne, 2002) has altered flow patterns and heating patterns within the basin, and several hydroelectric projects increase T_w (OR DEQ, 2006). Logging within the watershed reduces shading and also increases T_w (Johnson & Jones, 2000). ~~deforestation of the riparian corridor (decreased shading) (Gregory et al. 1991, Wallick et al. 2022), water diversions, and storage for agriculture have also likely shifted T_w (Berger et al., 2004) and several hydroelectric projects increase T_w (OR DEQ, 2006).~~ Nonetheless, summertime peak T_w values at reservoir sites likely decreased after dam construction, because of increased water depths; at the same time, autumn temperatures have increased (e.g., Angilletta et al., 2008; Rounds, 2010). Below the storage reservoirs, channelization of the Willamette, ~~deforestation of the riparian corridor (decreased shading) (Gregory et al. 1991, Wallick et al. 2022), water diversions, and storage for agriculture have also likely shifted T_w (Berger et al., 2004).~~ Because of a lack of in-situ data from pre-reservoir conditions, the cumulative effect of anthropogenic influence since European settlement is currently unknown (OR DEQ, 2006).

Hydrological and land-use changes in ~~temperate-zone river basins~~ the Willamette Basin have occurred within a background ~~are occurring simultaneously with~~ of a warming climate marked by ~~and~~ hotter extremes (e.g., Cloern et al., 2011; Hamlet & Lettenmaier, 1999; Palmer et al., 2010). ~~FAir Temperature (T_a) values in the Pacific Northwest have~~ warmed about ~1.1 °C since 1900 (Mote et al., 2019), ~~and~~ ~~t~~ The summers of 2009, 2015, and 2021 ~~were had~~ dry and hot in the Pacific Northwest ~~hot~~, with conditions consistent with the future climatology predicted by predictions from climate models (e.g., Mote and Salathé, 2010; Bumbaco et al., 2013). In 2015, snow pack was extremely low, leading to record low streamflow in many rivers (Mote et al., 2016). The combination of hot, dry weather and low river discharge (Mote et al., 2016) produced elevated T_w ~~water temperature values in 2015~~, adversely affecting salmon populations (Crozier et al., 2020). ~~Extreme~~ However, despite record air temperatures, however, do not always lead to extreme T_w , for reasons we investigate, ~~heat waves during the summer of 2021 (Portland reached a record air temperature of extreme 46.7 °C, about 5 °C above the previous all time high), water temperatures in the Willamette River, a major tributary of the Columbia River, did not reach the peak of 2015.~~

Formatted: Font: (Default) Times New Roman, 12 pt

Formatted: Font: Italic

Formatted: Font: Italic, Subscript

Formatted: Not Highlight

Formatted: Highlight

Anomalously hot years are useful for understanding processes that control T_w , and characterizing natural variability in the context of climate change.

Formatted: Font: Italic

In this manuscript we investigate whether T_w averages and extremes over the How anomalous were water temperatures in coastal rivers in the Pacific Northwest during 2009, 2015 and 2021 past 20 years are significantly different than late 19th and mid-20th-century conditions, using a much longer T_w record than previously available. From multiple, previously forgotten and neglected sources we, and to what extent has climate change influenced extremes? How much have water temperatures changed from natural, background conditions? The dearth of long-term data complicates assessment of patterns and trends, since weather patterns such as El Niño/La Niña and the Pacific Decadal Oscillation influence interannual and decadal variability in T_w (Peterson & Kitchel, 2001). Also, the construction of reservoirs, deforestation of the riparian corridor, irrigation diversions, and other land-use changes are known to influence flow hydrographs and T_w in other basins (e.g., Olden & Naimen, 2010). Because chronic and acute anthropogenic factors change over time, they may mask or accentuate climate-induced variability and trends in degradation or recovery (NASEM 2022).

Formatted: Superscript

Formatted: Superscript

Formatted: Subscript

To investigate the secular changes in water temperatures caused by climate change and local anthropogenic influence, we construct a unique, instrument-based T_w data set on the lower Willamette River (OR) that extends back to 1881, a time period with a cooler climate and unimpeded, natural flows, before the onset of irrigation in the basin. Water temperature records were found and digitized from various federal, state, and local archives, producing 90 years of daily records stretching over a 140-year period. Seasonal patterns and long-term trends are assessed, and their relationship to local air temperatures are evaluated using We used a stochastic regression approach is used to infill data gaps back to 1850, and statistical models from different eras are used to attribute changes to either climate change or local factors. Results show that extreme summertime water temperatures similar to 2009 and 2015 are found in the historical record (e.g., 1889 and 1941), and that water temperatures have frequently exceeded 20°C during the summer, even in the 19th century. However, on secular time scales, average water temperature is rising during all times of the year. Our combined archival research and statistical approach provides insights into how and why temperatures are increasing in coastal rivers like the Willamette, with implications for the future response of T_w water temperature zone in to the climate change, and the number of warm water days is increasing. Therefore, temporal refugia during the time periods most conducive to cold water species are becoming increasingly scarce.

2. Background and Methods

2.1 Study Area Setting

The Willamette River (Figure 1), with has a 1971–2020 mean annual discharge of 940 m³/s (1971–2020 period) and, drains approximately 29,700 square km² of coastal Oregon (Figure 1; Branscomb et al., 2002). It is the 13th largest river in the contiguous United States by volume (Wallick et al. 2022), and its waters discharge into the larger Columbia River approximately 162 km from the Pacific Ocean. The lower Willamette River, the focus of this study (Figure 1), is an approximately 43 km long, region. It is influenced by ocean tides most of the year, during low

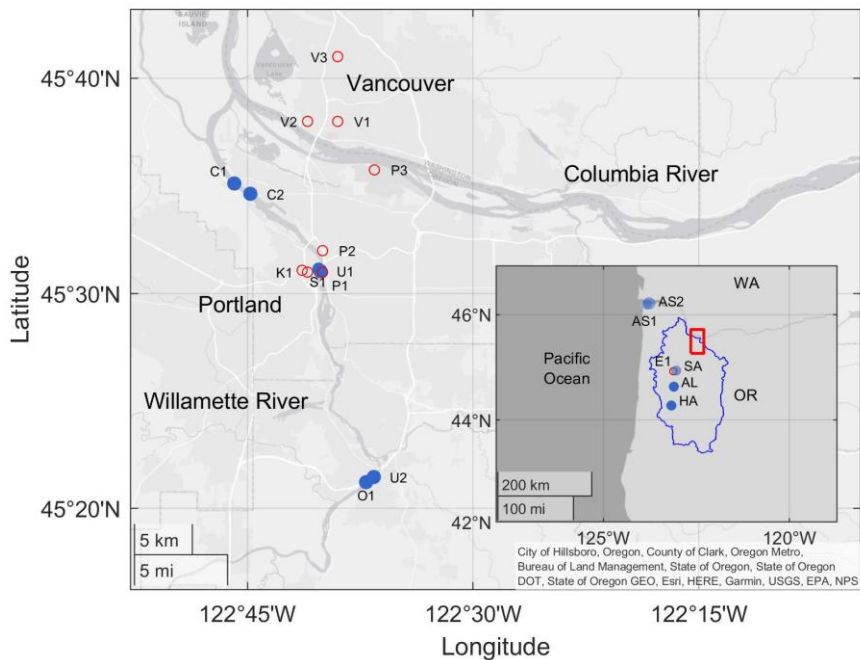
Formatted: Superscript

197 ~~flow conditions~~ and by backwater from the Columbia River, particularly during spring (Helaire
198 et al., 2019). Because of its location near the mouth, the lower Willamette is influenced by, and
199 integrates climate changes and local anthropogenic changes ~~occurring throughout the~~ within, its
200 ~~entire~~ basin.

201 Evaluating changes to T_w in the Lower Willamette River is important because it influences the
202 long-term viability of salmon and other vulnerable and endangered species (Mantua, 2010; Bot-
203 tom et al., 2011, Isaak et al., 2012, Caldwell et al., 2013; Clemens 2022). Above a threshold of
204 18–21 °C, various species of salmon, steelhead, and trout are stressed and become more suscepti-
205 ble to disease (OR DEQ, 2006, Mantua, 2010). Also, the migration and spawning of Willamette
206 River fish such as Pacific lamprey (*Entosphenus tridentatus*) (Clemens et al. 2016) and Chinook,
207 coho, and chum salmon (Richter and Kolmes 2005) are directly impacted by elevated tempera-
208 tures. Because of such ecological effects, regulations require that the seven day average of the
209 daily maximum temperature should not exceed 20 °C, with a lower threshold set for rearing and
210 spawning streams (e.g., OR-DEQ, 2006).

211
212 ~~Their net effect on T_w is explored in this manuscript; here, we first review the time history and~~
213 ~~magnitude of anthropogenic changes.~~

Formatted: Not Highlight



214

Figure 1: Site map with locations of T_w (blue, closed circles) and T_a (red, open circles) measurements. The red bounding box in the inset denotes the Portland/Vancouver Metropolitan Area depicted in the larger figure. The Willamette River watershed boundaries are denoted in blue. OR = Oregon, WA = Washington. Abbreviations and period of record of the measurements are provided in Table 1.

Formatted: Space After: 18 pt

The Willamette Basin has a temperate climate marked by overcast conditions from October–May, and predominately sunny, dry conditions from approximately mid-June to mid-September. Average annual precipitation on the valley floor is ~ 100 – 130 cm/yr., with up to 500 – 5 cm occurring in the Cascade Mountains mountainous headwater areas (Baker et al., 2002). Rainfall and high discharge events occur primarily between October and May, with the wettest period occurring between November and March/January. At Portland, the largest discharge typically occurs during winter storms and peaks in the November–February period (Figure 2a). Historically, snow-melt-driven flows contributed to elevated flows in the March–May time frame (Figure 2a). The, but a combination of declining snowpack (e.g., Mote et al., 2018) and water management (e.g., Rounds, 2010) has reduced spring discharge (Mote et al., 2018; Rounds, 2010). During summer, 60–80% of river water derives from high-elevation regions above 1200m, either as direct snowmelt or as groundwater (Brooks et al., 2012). Late-summer discharge has increased, however, because of the managed release of water. In the future, unimpeded unimpeded discharge is wintertime discharges are expected to increase in winter and while summertime flows decrease in summer (e.g., Chang & Jung, 2010).

Formatted: Highlight

The mainstem of the Willamette River, which runs 300km south-to-north, has been extensively modified since the latter part of the 19th century, first for navigation and agriculture, and later for flood control. The lower 300km of the Willamette River runs south to north through the Willamette Valley, which is now primarily agricultural. For thousands of years the Willamette Basin was inhabited by Native Americans, who influenced the watershed in many ways, including through controlled burns and small scale fish dams (Boyd, 1999; Johannessen et al. 1971; Taylor, 1999). European settlement began in the early 1800s; Portland, founded in 1843, became the largest city in Oregon by 1860 (US Census, 1866). Shading has been reduced in its modern, channelized configuration compared to historical norms (Lee et al. 1995; OR-DEQ 2006). Land under irrigation was minor before 1910, and but increased almost tenfold from $\sim 13,500$ to hectares in 1945 to about 110,000 hectares by 1979 (Sedell & Froggatt, 1984). East side tributaries such as the Clackamas River (Willamette Rkm 40), the Molalla River (Rkm 58) and the McKenzie River (Rkm 282) drain the mountainous Cascade Range, and flow primarily through steep forested regions. West side tributaries such as the Tualatin River (Rkm 45) and the Long Tom River (Rkm 240) drain the lower, forested Coast Range and are slower moving (Lee et al., 1995). The Willamette splits into the Middle and Coast fork at Rkm 301; the headwaters of the Middle fork are approximately 486km from the confluence of the Willamette and the Columbia rivers.

The mainstem of the Willamette River has been extensively modified since the latter part of the 19th century, first for navigation and agriculture, and later for flood control. Pre-Before European settlement, the river was maintained in a prairie or savannah-like condition by burning (Christy and Alverson 2011). After burning ceased (late 1700s), the river became fringed by a 3–7 km wide floodplain covered by a dense riparian forest and 2–5 shallow, braided channels (1.5–3m

depth) that evolved each year (Thilenius 1968, Sedell & Froggatt, 1984; Gregory et al., 2002a; Wallick et al. 2022). In the 1850s, approximately 97,500ha of the Willamette Valley was mapped by the Government Land Survey Office as riparian and wetland forest, and was dominated by tree species such as *Quercus garryana* (Oregon white oak), *Fraxinus latifolia* (Oregon ash), *Acer macrophyllum* (bigleaf maple), *Alnus rubra* (red alder), and *Populus trichocarpa* (black cottonwood) (Christy and Alverson 2011). The river planform was dynamic; the upper 200km typically contained 2–5 shallow (1.5–3 m deep), braided channels that evolved each year due to the formation of gravel bars and driftwood barriers (Sedell & Froggatt, 1984; Gregory et al., 2002a; Wallick et al. 2022). Beginning in the 1870s, but particularly in the first half of the 20th century, the river was reduced to a primarily single-thread stream, and shortened by nearly 20km (Sedell & Froggatt, 1984; Gregory et al., 2002a). Shading was much reduced (Lee et al. 1995; OR-DEQ 2006). Bank-stabilization measures began in the late 1800s and occurred most prominently during the mid-20th century (1930s–1960s); approximately 25% of Willamette River banks now have revetments, armoring, wing dikes, and other bank engineered protection measures (Gregory et al., 2002b). Further, from 1870–1950, approximately 65,000 “snags” dead trees (30–60m long trees with a diameter of 0.5–2m) were removed (>500 per km; Sedell & Froggatt, 1984). Peak snag removal occurred in the late 1800s/early 1900s (Sedell & Froggatt, 1984). These snags were often used to block up side channels. As a result of these efforts, off-channel areas such as alcoves and sloughs—often 2–7 °C cooler than the mainstem—have decreased in extent by 70–80% (Landers et al., 2002). Additionally, the forested floodplain area in the floodplain has decreased by 75–90% (Landers et al., 2002, Gregory et al. 2019). Dredging further altered the river upstream of ~Rkm 50, after its authorization in 1906 particularly before 1930. Between 1908–1929, approximately 78,000 m³·yr⁻¹ of sediment were removed from the river above tidewater (Willingham, 1983); and, but much more extensive dredging has occurred in Portland Harbor (e.g., Helaire et al., 2019). The depth of the river is currently ~12m in the lower ~20km of the Willamette, the focus area of our study (Figure 1). Depths gradually reduce to a centerline depth as shallow as 1.5–2m around Rkm 280 (US Geological Survey (USGS), 2003).

A total of 371 reservoirs and impoundments of various size have been built in the Willamette basin, with a combined capacity of more than 3.3 km³ (Payne, 2002). Given a mean discharge of about 980 m³·s⁻¹ (Naik and Jay, 2011), these reservoirs potentially store ~10.6% of the annual average flow. The majority were built between 1950–1980, with only ~23 built pre-1950 and ~25 after 1980 (Payne, 2002). Approximately 45% are small storage reservoirs for irrigation (order 100,000 m³ capacity); hydroelectric dams (~9%) and water supply reservoirs (6% of total) are typically of similar size (Payne, 2002). A total of 13–14 federal reservoirs for storage and flood control reservoirs were built between 1941–1953 and 1969 with a combined maximum storage capacity of 2.75–57 km³ (Rounds, 2010); the largest are Detroit Dam (completed 1953, capacity 0.56 km³), Lookout Point Dam (completed 1954, capacity 0.59 km³) and Green Peter Dam (0.53 km³ capacity, completed 1968; Payne, 2002; Rounds, 2010). The two federal reservoirs built in the 1940s were relatively small (combined capacity of 0.18 km³) compared to modern capacity; therefore, we consider the period before 1953 to be pre-river flow regulation. An examination of hydrological records suggests that flood control exerted some influence in the 1954–1964–1969 period, reducing peak flows during the December 1964 flood considerably; thus, the modern hydrological regime began ~1965–1970 during this period (Waananen et al. 1970; Gregory et al., 2002c).

~~In total~~, reservoirs have increased the surface area of water within the system by about 200 km², with the majority (80–85%) occurring in the 13 federally operated water projects (Payne, 2002). ~~An additional~~ net increase of ~50 km² in water surface area is estimated for the Willamette Valley since 1851 (Gregory et al., 2002d), in part from water impoundments. By comparison, channelization between 1850 and 1995 ~~only~~ removed ~ 17 km² of water surface on the mainstem Willamette, from 76 to 59 km² (Gregory, 2002a). ~~Combined with the loss of riparian corridor shading during the growing season (Gregory et al., 2002e; Rounds, 2007), the increased surface area in the basin means that heat input into the fluvial system—for given the same constant meteorological conditions—has increased.~~ Summertime peak T_w values at reservoir sites are hypothesized to have decreased after dam construction; at the same time, autumn T_w ~~water temperatures have~~ increased (e.g., Angilletta et al., 2008; Rounds, 2010).

Formatted: Space After: 24 pt

Formatted: Not Highlight

Formatted: Not Highlight

Formatted: Not Highlight

2.2 In-situ water temperature measurements

~~A number of m~~Measurements were obtained ~~from~~ multiple federal, state and local archives and databases to assess ~~changes to~~ meteorological and fluvial conditions ~~since the mid-19th century between 1850–2021 (Figure 1; Table 1 & Table 2), and approximately 30 years of archival records were digitized.~~ We found and digitized previously unused and forgotten records from ~~From 1881–1890, the US Signal Service (1881-1890 USSS) and measured top and bottom T_w at Portland at 11:00 (local time) every day. The successor to the USSS, the US Weather Bureau (USWB) measured T_w from (1941–1961) held at the between 6:30 am and 7:30 am daily (local standard time). We digitized and quality assured the previously unanalyzed USSS and USWB records, which were obtained from the~~ National Centers for Environmental Information (NCEI). A spot-check of US Army Corps of Engineers records from Willamette Rkm 10.5 from 1941– 42 (Moore, 1968) showed a general consistency with ~~individual~~ USWB measurements, to within 1° C. ~~Modern records of Measurements of T_w are available from the US Geological Survey (USGS) since 1961, with ~26 station years available in the Portland metropolitan area since 1971 (Table 1). Such-These~~ federal records are supplemented by additional state and local records. ~~Intermittent g~~Grab-sample measurements of T_w are available from the State of Oregon Department of Water Quality, particularly during summer (1949, 1953–present; obtained from the City of Portland). ~~Additionally, n~~Nearly continuous daily measurements of T_w at the Willamette Falls fish ladder from 1985– 2020 were obtained from the Oregon Department of Fish and Wildlife. Finally, ~~a long, continuous record has been made available by the City of Portland was were obtained at half hourly increments from for 1992–1999 and 1997–2015 at the Saint Johns Bridge and the St Johns Railroad Bridge, respectively two locations near Portland (City of Portland; see also Annear et al., 2003).~~

We combined the above T_w ~~water temperature records from these different locations are combined together herein~~ to obtain a 90-year record of in-situ T_w covering 64% of the 1881 to 2021 period

(Table 1). ~~Once-a-day~~Daily measurements were adjusted to the daily minimum temperature, because most historical measurements were made in the morning. The adjustment, typically ~0.1 °C, was based on the monthly averaged differences between measurement time stamps and the daily minimum in modern, high resolution data (Table 1). The composite 1881–2021 record uses Lower Willamette records when available, and the nearest mainstem data otherwise (if available). Records in Oregon City and ~~far~~ further upstream were adjusted for spatial heating effects through the use of monthly averaged gradients observed between coterminous measurements from 2000–2017. Most adjustments for spatial variability were minor (<0.3 °C), except for ~~a few years (1962– and 1983–1984), in for~~ which the only available measurements were from the middle or upper Willamette River. Additional notes are included in Table 1, and the sources of data in the composite are included in the data record (see data repository supplement).

Additionally, we use T_w measurements from the lower Columbia River to check our model estimates (see section 2.4) during periods with no other data (Figure 1, Table 1). ~~T_w Water temperature~~ was measured up to twice daily at Astoria, approximately 24 km from the ocean, from 1854–1876 (Talke et al., 2020), ~~approximately 24 km from the ocean present-day mouth~~. Monthly estimates of T_w at ~~Astoria~~, Tongue Point (Rkm 29) are available from 1925–1964 (U.S. Coast and Geodetic Survey (USC&GS), 1967), and daily records were obtained from 1940–42 (Moore, 1968) and 1949–present from the National Oceanographic and Atmospheric Administration. Before 1950, surface waters at Astoria were generally freshwater or brackish during typical flow conditions (Al-Bahadily, 2020, USC&GS, 1967), and therefore ~~approximate are representative of river T_w values river water temperatures~~. ~~During the November–April rainy season, good agreement is found between model results and Astoria measurements, thus helping to validate the model. During other times of year, snow melt from the interior Columbia River basin dominates the river flow signal (e.g., Naik & Jay, 2011; Helaire et al., 2019), suppressing water temperature (see Results, Section 3). Additional information about the Astoria measurements is given in Talke et al. (2020) and Scott et al. (2022).~~

The availability and quality of in-situ data informs our choice of model calibration periods and interpretation of model/data comparisons, as described in the following examples. Monthly averages of the USGS, DEQ, and City of Portland data from 2009 to 2015 agree to within 0.1–0.2 °C, indicating that modern measurements from the last two decades are consistent and of high quality. This comparison also shows that grab samples from the water surface compare favorably with other methods. Measurements by the USSS (1881–1890) and USWB (1941–1961) were made at a 1st-order weather station by trained professionals, and appear to be of high quality; however, little independent verification is possible. Evaluation of data from 1962 to the mid-1990s indicates some periods with lesser quality in which different measurements disagree with each other. For example, summertime measurements from a thermograph in Oregon City (1963–1967) are as much as 1.8 °C higher (monthly average) ~~with than~~ coterminous grab-samples; a smaller, ~~but still significant, bias is found difference occurs~~ between Saint Johns Bridge measurements (1971–1975) and grab-samples (Table 1). ~~Since-Because~~ the typical difference between such measurements is reported to be <1 °F (0.56 °C) (Moore, 1967), ~~some unknown undocumented instrumental or measurement~~ issue occurred. ~~The availability and quality of in-situ data informs our choice of model calibration periods and interpretation of model/data comparisons.~~

Formatted: Highlight

Table 1: In-situ T_w water temperature measurements used to obtain a composite record of daily minimum water temperature in Portland, 1881–2021. Locations ordered based on start-date and originating agency. Precision based on measurement significant figures. A bias correction was applied to standardize measurements to the daily minimum T_w , based on the time of day of the measurement, and to account for the T_w water temperature gradient between Portland and upstream stations. River kilometers (km) from the mouth are indicated for the Columbia River (CR) and the Willamette River (WR). Additional information on the data used in the composite in situ T_w series is included in the data repository.

Location	Originating agency	Short name	River km	Latitude	Longitude	Measurement Dates	Measurement Frequency	Precision	Bias Correction	Dates used in composite T_w
Astoria Downtown ^a	US Coast Survey	A1	CR-24	46.19	-123.829	6/1854–10/1876	Various, usually 6:00 am and 6:00 pm daily	±0.03 °C	None applied	
Stark Street, Portland ^b	US Signal Service	S1	WR-21	45.519	-122.671	9/1881–11/1890	11:00 am daily	±0.3 °C	0.1 °C to 0.2 °C	1881-1890
Astoria Tongue Point	US CGS (pre-1973) & NOAA	A2	CR-29	46.207	-123.768	1/1925–present; daily to 1995, hourly 1995–present	Monthly 1/1925–12/1964; Daily 11/1940–6/1942, 01/1949–12/1995; Hourly 11/1993–present	±0.2 °C before 1994; ±0.03 °C modern	None applied	
Morrison Street Bridge, Portland ^b	US Weather Bureau	W1	WR-21	45.517	-122.668	7/1941–10/1961	7:30 am daily (except Sunday)	±0.3 °C	0 °C to 0.2 °C	1941-1961
Lower Willamette River ^d	Oregon Department of Environmental Quality	D1	WR-19–21 (primarily)	Various	Various	1949–2015; 2746 grab samples retained after quality assurance	6:00am–12:00 pm; mode = 9:00 am. monthly in winter, once weekly in summertime	±0.1 °C	Median 0.1 °C; 90% corrections < 0.2 °C	1963-1974
Harrisburg	USGS Gauge 14166000		WR-259	44.2704	-123.174	6/1961–9/1987 10/2000–Present	Daily Max, Min & Mean	±0.05 °C	Spatial gradient correction, June–September	1961-1963, 1982-1984
Oregon City	USGS Gauge 14207770	U2	WR-42	45.3578	-122.610	3/1963–9/1967	Daily Max, Min & Mean	±0.05 °C	0.7–1.8 °C Diff. w/Grab samples during summer	1963-1967
Salem	USGS Gauge 14191000	SA	WR-137	44.9442	-123.0429	10/1963–9/1987	Daily Max, Min & Mean	±0.05 °C		1981-1982
Saint Johns Bridge	USGS Gauge 14211805	U3	WR-9	45.583	-122.759	10/1971–9/1975	Daily Max, Min & Mean	±0.05 °C	0.6–1.05 °C Diff. w/Grab samples during summer	1971-1975
Morrison Street Bridge, Portland	USGS Gauge 14211720	U1	WR-21	45.5175	-122.669	11/1975–9/1981 11/2001–9/2005 01/2009–Present	Daily Max, Min & Mean through 2005. Every 30 minutes	±0.05 °C	None applied	1975-1981; 2001-2005; 2009-2021
Willamette Falls Fish Ladder ^e	Oregon Department of	O1	WR-43	45.354	-122.618	01/1985–present	Not tabulated; Daily, with gaps	±0.2 °C	-0.3 to 0.3 °C, based on monthly difference with Portland	1985-1999; intermittently thereafter

Formatted: Space After: 12 pt
Formatted: Subscript
Formatted: Section start: New page
Formatted: Subscript

Formatted Table
Formatted: Font: Italic
Formatted: Font: Italic, Subscript
Formatted: Not Highlight

Formatted: Not Highlight

Formatted: Not Highlight

Formatted: Not Highlight

Formatted: Not Highlight

Formatted: Not Highlight

Formatted: Not Highlight

Formatted: Not Highlight

Formatted: Not Highlight

	Fish and Game									
Saint Johns Bridge^f	City of Portland, BES	C1	WR-9	45.585	-122.765	7/1992 – 9/1999	Every 30 minutes	± 0.01 °C	Very biased; not used.	
Saint Johns Railroad Bridge^f	City of Portland, BES	C2	WR-11	45.5773	-122.747	9/1997– 9/2012 2015	Every 15 minutes	± 0.01 °C	Averaged with USGS record	1999-2012
Albany	USGS Gauge 14174000	AL	WR-192	44.6388	-123.107	08/2001– Present	Daily Max, Min & Mean	±0.05 °C		

Notes: Stations ordered by start date, with earliest measurements first. All times given in local standard time. Bias corrections are subtracted from raw measurements on a monthly basis to obtain daily minimum; a positive value indicates a downward adjustment. Coordinates provided in the North American Datum of 1983. The locations for the measurements at Stark Street, Astoria Downtown, Willamette Fish ladder and the City of Portland measurements are estimated based on available data. River km are the thalweg distance from the mouth of the Willamette, except for Astoria which is on the Columbia River.

Specific Footnotes: (a) Measurements obtained from US National Archives; see Talke et al., 2020; (b) Measurements obtained from National Centers for Environmental Information; (c) Data obtained from NOAA; Grab samples from 1925–1995, approximately daily, generally between 10:00am–1:00pm; median ~11:30 am.(d) Data obtained from US EPA Storet database. Measurements often made from bridges in the Portland Metro area, including the Hawthorne Bridge, the Steel Bridge, and SPSS Railway Bridge. Samples pre-1960 discarded because of lack of time stamp. Grab samples after 12:00 pm (noon) not considered to avoid afternoon heating signal. Pre-12:00 pm data adjusted to daily minimum on monthly basis based on modern USGS data. Measurements at 1–3 day frequency in 1964–1972; (e) Data from 1985–1999 obtained directly from agency; post 1999 records available online. Based on a comparison using 2001-2004 data, an average warming of 0.2 to 0.3 °C occurs between Willamette Falls and Portland from July to September. A cooling of up to 0.3 °C occurs between March to May. Little variation occurs at other times; (f) Obtained directly from agency; pre-2000 data also obtained from Berger et al., 2004.

Formatted: Not Highlight

Formatted: Not Highlight

A nearly complete ~~record of USGS~~ discharge ~~in record for~~ the lower Willamette River is available from 1893–~~to~~ present, with ~~less certain intermittent value estimates~~ available from 1878–1892. Daily discharge is available from the USGS in Portland from 1972 to the present (USGS Gauge 14211720). Routed estimates of discharge at Portland are available for earlier periods from 1878 forward from Jay & Naik (2011), based on USGS measurements at Albany (USGS Gauge 14174000) and Salem (USGS gauge 14191000). ~~Routed estimates pre 1893 are less certain, because of gaps in the record (Jay & Naik, 2011). Daily Portland water level measurements are available from 1876–present, and estimates of 30d averaged Portland water level are available from 1855–1876 based on tidal measurements at Astoria (Talke et al. 2020). Nineteenth century measurements incorporate a substantial backwater effect from the Columbia River that historically varied from zero to as much as 10 m during some the largest spring freshet events (see Helaire et al., 2019).~~

Records of daily maximum T_a from the Portland-Vancouver area were found in several sources (Table 2). ~~Continuous d~~Daily ~~USSS~~ weather records at Vancouver (1849–1868) and Eola (1870–1892) ~~were measured by the USSS and~~ were provided in digital form by the Midwestern Regional Climate Center (<https://mrcc.purdue.edu/>). Additional daily records from the USWB and the National Weather Service from Portland and Vancouver cover the 1874–present period and were obtained from NCEI.

Air temperature (T_a , Air temperature records) records were carefully evaluated for potential bias (e.g., caused by elevation differences) and consistency with each other (Table 2; see Figure 1 for locations). For example, the Vancouver record from 1895–1965 ~~is on an average~~ is on average ~ 0.4 to 0.5 °C warmer than the downtown Portland record. ~~The Average Portland Airport reading was values were~~ The Average Portland Airport reading was values were < 0.05 °C cooler than the downtown Portland Weather Bureau readings between 1940–~~and~~ 1948, ~~on average~~. Thereafter, the downtown Portland ~~Weather Bureau~~ record warmed more quickly, and was 0.54 °C warmer than the Airport from 1960–1969. The modern Portland KGW record (1973–present), located at 48.5m above sea-level, is slightly cooler from 1991–~~to~~ 2020 (annually averaged daily maximum = 17.08 °C) than the Portland Airport (17.47 °C). Under standard atmospheric conditions, with a lapse rate 6.5 °C per 1000m, a difference of ~ 0.3 °C is expected between these records as compared to the actual difference of 0.39 °C. Thus, we conclude that the measured difference between the stations is almost entirely explainable by elevation effects. After adjusting for mean biases, the root-mean-square error (RMSE) error observed between the ~~different various daily~~ Portland T_a ~~air temperature~~ records is around about 1 – 1.1 °C from 1940–present. ~~Comparison of The RMSE-D daily maxima between between~~ Vancouver and Portland T_a ~~show is are more variability larger (RMSE of 1.5 – 1.6 °C)~~, possibly because of small differences in local climate. The influence of these small differences on our T_w model results ~~are is~~ explored later.

Table 2: Meteorological stations used to develop statistical models, and associated root mean square error (RMSE) of T_w water temperature obtained for different calibration periods (annual, summer, and winter). The RMSE represents either the daily or monthly averaged difference with in-situ T_w water temperature measurements, in degrees Celsius. Station Identification numbers (ID) are from the US National Weather Service. Measurement dates denote the time period that daily maximum temperature was recorded at the given location. The latitude/longitude value for Eola (near Salem, Oregon) is estimated. All stations except Vancouver are in Oregon.

Formatted: Section start: New page

Formatted Table

Model Name	Air temperature dataset used in modelName	Station ID	Measurement DatesDates modeled	latitude	longitude	Calibration Period	RMSE Annual Calibration (°C)	RMSE Summer Calibration (°C)	RMSE Winter Calibration (°C)	RMSE Annual (monthly avg) (°C)	RMSE Summer (monthly avg) (°C)	RMSE Winter (monthly avg) (°C)
1881D	Portland Downtown	USW00024274	1874–1902	45.5166	-122.6667	1881–1890	1.1	1.2	0.87	0.78	0.92	0.5
1941D	Portland Downtown	USW00024274	1902–1973	45.5333	-122.6667	1941–1952	0.91	0.68	0.75	0.62	0.48	0.43
1941A	Portland Airport	USW00024229	1938–2021	45.5958	-122.6093	1941–1952	0.91	0.66	0.78	0.6	0.46	0.42
2000A	Portland Airport	USW00024229	1938–2021	45.5958	-122.6093	2000–2015	0.88	0.51	0.75	0.62	0.31	0.48
2000D	Portland KGW ²	USC00356749	1973–2021	45.5181	-122.6894	2000–2015	0.87	0.53	0.72	0.62	0.33	0.46
1941V	Vancouver, Washington ³	USC00458773	1849–1868 1891–1966	45.6333	-122.6833	1941–1952	0.98	0.75	0.85	0.68	0.54	0.48
1881E	Eola	US Signal Service Observation	1870–1892	44.9323	-123.1198	1881–1890	1.22	1.41	1.05	0.91	1.17	0.72

Formatted: Space Before: 12 pt, After: 0 pt

Formatted: Space After: 0 pt

Notes:

1. The annual RMSE between measurements and the climatological average is 1.86, 1.46, and 1.43 °C for the 1881–1890, 1941–1952, and 2000–2015 calibration periods, respectively.
2. The 1973–1999 measurement was at a slightly different location of (45.517W, -122.683E). The elevation of the 1973–present dataset is ~48.5m. The lapse rate for the standard atmosphere (6.5 °C per 1000m) suggests that the difference to a measurement at sea-level is ~0.3 °C. An observed difference in average daily maximum temperature at the Portland Airport (17.46 °C, <10m relative to sea-level) and Portland KGW (17.07 °C) between 2000–2020 is therefore mostly caused by elevation differences.
3. The Dec. 1849–1868 measurement at Fort Vancouver was made by the US Signal Service; the approximate location was 45.633N, -122.65E, and was several km east of the 1891–1966 measurement. The gauge was moved in 1966 to a higher elevation location with a known bias (Mote et al., 2002). The 1966–present data is therefore not used.

450

451

452 2.3 Advection-Diffusion equation

453 To develop our statistical model approach, understand its limitations, and motivate its form, we
 454 first consider the underlying physical dynamics. Heating and cooling of river water is governed
 455 by the Advection-Diffusion equation (ADE; e.g., Fischer et al., 1979). When vertical and cross-
 456 sectional variations in T_w are neglected, the 1-D ADE for T_w as a function of time t and along-
 457 channel coordinate x (positive downstream) reads:

$$458 \frac{\partial T_w}{\partial t} = \underbrace{-u \frac{\partial T_w}{\partial x}}_{\text{Advection Term}} + \underbrace{\frac{\partial}{\partial x} \left(K \frac{\partial T_w}{\partial x} \right)}_{\text{Diffusive Term}} + \underbrace{\frac{H}{\rho c_p d}}_{\text{Heating term}},$$

459 (1)

460 where K is a horizontal diffusion coefficient, u is river velocity, H is the sum of heat flux into or
 461 out of the system, d is the cross-sectionally averaged depth, ρ is the density of water, and c_p is
 462 the heat capacity of water, and is approximately constant to within 1% for typical variations in
 463 T_w . This simple ADE does not consider groundwater flow, which cools the off-channel alcoves
 464 of the Willamette River during summer (Faulkner et al., 2020).

465 We use scaling of Equation 1 to determine the relative importance
 466 of the advection, diffusion, and heating terms, relative to the time rate of change $\frac{\partial T_w}{\partial t}$. Over a
 467 12 hour time scale during the day, temperatures in summer are observed to vary by $\sim 0.5^\circ\text{C}$,
 468 yielding $\left(\frac{\partial T_w}{\partial t} \right)_{\text{daily}} \sim 10^{-5}^\circ\text{C/s}$. Over a month, larger changes of order 5°C are observed, yield-
 469 ing $\left(\frac{\partial T_w}{\partial t} \right)_{\text{monthly}} \sim 2 \times 10^{-6}^\circ\text{C/s}$. The time rate of change for daily and monthly time scales must
 470 be balanced by the terms on the right hand side of Equation (1). An evaluation of measurements
 471 suggests that the:

- 472 The diffusive term is negligible, but that, Over most of the year, the monthly average of
 473 daily $\frac{\partial T_w}{\partial t}$ is $\ll 10^{-5}^\circ\text{C/m}$, except from July–September when a monthly averaged increase of 1–
 474 2°C per 100km is observed (Figure 2b). Using 100km as a typical length scale and $K \sim 1000 \text{ m}^2/\text{s}$
 475 for the diffusive term, the $\frac{\partial}{\partial x} \left(K \frac{\partial T_w}{\partial x} \right)$ term is generally $< 10^{-7}^\circ\text{C/s}$, much less than $\frac{\partial T_w}{\partial t}$.
- 476 The nonlinear advective term is likely influential during summer, due to a positive $\frac{\partial T_w}{\partial x}$
 477 (Figure 2b). During other seasons, river discharge can either cool or warm Portland water be-
 478 cause of the presence of both negative and positive $\frac{\partial T_w}{\partial x}$ (Figure 2). Therefore, the net influence of

Formatted: Line spacing: Multiple 1.2 li

Formatted: Font: (Default) Times New Roman, 12 pt

Formatted: Space After: 6 pt, Line spacing: Multiple 1.2 li

Formatted

Formatted

Formatted

Formatted: Font: (Default) Times New Roman, 12 pt

Formatted: Normal, Space After: 6 pt, Line spacing: Multiple 1.2 li, No bullets or numbering

Formatted

Formatted

Formatted

Formatted

Formatted

the advective term on monthly averaged temperatures is likely small, though it may matter during weather events (such as a rain-on-snow event).

Seasonal variations in discharge (Figure 2a) influence the magnitude of the advective term. Nonetheless, the low velocities in late summer counteract the influence of large Q . During early summertime (June) conditions, Lee (1995) measured velocities of ~ 0.8 m/s in the upper Willamette; tidally averaged currents are typically 0.05–0.1 m/s during the same period in Portland (USGS Gauge 14211720). Since discharge is smallest during August/September, the decrease in u counteracts the increase in $\frac{\partial T_w}{\partial x}$ in the advective term $u \frac{\partial T_w}{\partial x}$. Overall, considering typical magnitudes of u and $\frac{\partial T_w}{\partial x}$, we find that the advective term scales as 10^{-5} °C/s to 10^{-6} °C/s during the summer, depending on location.

Based on our scaling on the considerations above, the heating term is usually the leading order term that drives the time rate of change of T_w , as also found, for example, by (c.f.,) Wagner et al., (2011). When advection and diffusion are unimportant, the non-linear heating term ($\frac{H}{\rho c_p d}$) governs the time rate of change of temperature, $\frac{\partial T_w}{\partial t}$. This $\frac{H}{\rho c_p d}$ term can be linearized, enabling use of a linear regression approach in which T_w is a function of T_a and river discharge Q (see Mohseni & Stefan, (1999) or the supplement for a more detailed discussion of linearization assumptions). The river discharge term incorporates the net influence of precipitation, snowmelt, and groundwater recharge.

Formatted: Font: (Default) Times New Roman, 12 pt

Formatted: Font: (Default) Times New Roman, 12 pt

Formatted: Font: 12 pt

Formatted: Font: 12 pt

Formatted: Font: 12 pt

Formatted: Font: 12 pt

Formatted: Font: (Default) Times New Roman, 12 pt

Formatted: Font: 12 pt

Formatted: Font: 12 pt

Formatted: Font: 12 pt

Formatted: Font: 12 pt

Formatted: Font: 12 pt

Formatted: Font: 12 pt

Formatted: Font: (Default) Times New Roman, 12 pt

Formatted: Font: 12 pt

Formatted: Font: 12 pt

Formatted: Font: 12 pt

Formatted: Font: 12 pt

Formatted: Font: (Default) Times New Roman, 12 pt

Formatted: Normal, Space After: 6 pt, Line spacing: Multiple 1.2 li

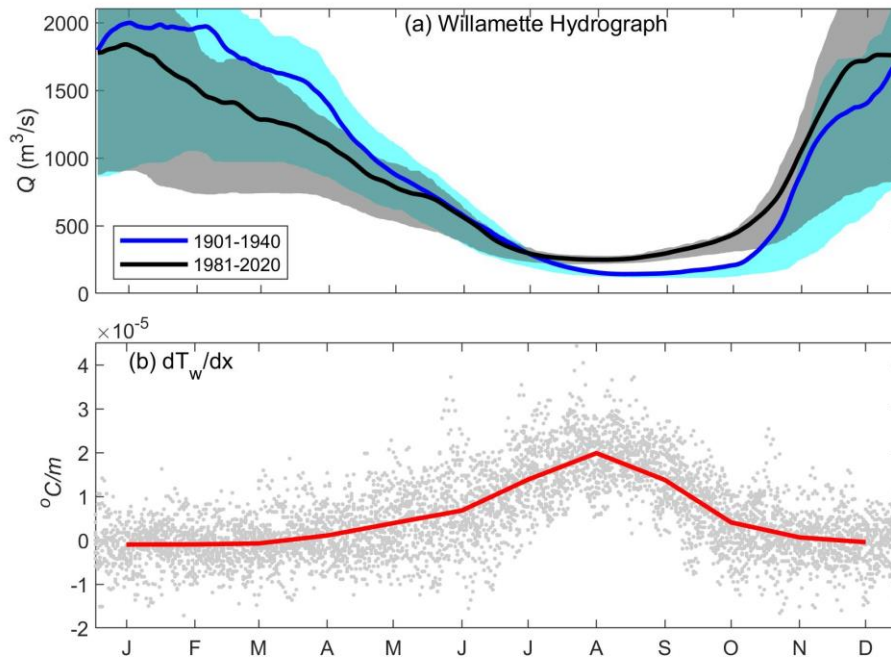
Formatted: Normal, Space After: 6 pt, Line spacing: Multiple 1.2 li, No bullets or numbering

Formatted: Font: (Default) Times New Roman, 12 pt

Formatted: Font: (Default) Times New Roman, 12 pt

Formatted: Font: (Default) Times New Roman, 12 pt

Formatted: Font: (Default) Times New Roman, 12 pt



499

500 Figure 2: (a) The Willamette hydrograph at Portland, Oregon for the pre-reservoir (1901–1940) and
 501 modern (1981–2020) periods, and (b) the horizontal T_w gradient between Albany, Oregon and Portland
 502 Oregon for the 2000–2017 time period. Positive indicates that downstream measurements in Portland
 503 are warmer. Shading in (a) denotes the 25th and 75th percentile of measured discharge. The along-river
 504 distance between Portland and Albany is 169 km. The red line in (b) denotes the monthly average. Tick
 505 marks denote the middle of each month.

Formatted: Space After: 18 pt

506

507 ~~When advection and diffusion are unimportant, the non-linear heating term ($\frac{\partial T_w}{\partial t}$) governs the~~
 508 ~~time rate of change of temperature, $\frac{\partial T_w}{\partial t}$. The $\frac{\partial T_w}{\partial t}$ term can be linearized using a number of as-~~
 509 ~~sumptions, enabling use of a linear regression approach in which T_w is a function of T_r and river~~
 510 ~~discharge Q . The details, described briefly below, reveal some inherent limitations. See~~
 511 ~~Mohseni & Stefan (1999) for a more detailed discussion of linearization assumptions.~~

512

513 First, we make the approximation that the reciprocal of depth, $1/d$, is a function of Q :

$$\frac{1}{d} \approx a_1 - a_2 Q, \quad (2)$$

where a_1 and a_2 are constants. The negative sign reflects the observation that $1/d$ decreases (depth increases) as discharge Q increases.

Further, the heat flux term is a function of at least 5 different terms (e.g., Fischer et al., 1979):

$$\Sigma H = H_s + H_e + H_{LW, gain} + H_{LW, loss} + H_{SW}. \quad (3)$$

The sensible heat flux is proportional to the difference between air temperature T_a and T_w (both measured in Celsius):

$$H_s = k_L w (T_a - T_w), \quad (4)$$

where k_L is a constant that depends on air density and several empirical coefficients, and w is the wind speed at 10m. The energy loss because of evaporative heat flux, H_e , depends on wind speed, the latent heat of evaporation, and atmospheric conditions, and is generally small in winter but potentially significant in summer (Wagner et al., 2011). The third term, the heat input from radiation from water vapor, is

$$H_{LW, gain} = k_{LW, gain} (273.15 + T_a)^6 \propto k_{LW, gain} T_a, \quad (5)$$

Where $k_{LW, gain}$ is a constant that depends on cloud cover. When ΔT_a is small relative to $(273.15 + T_a)$, such as occurs in the Willamette, Equation 5 is approximately linear with respect to T_a . Similarly, heat loss due to long-wave radiation is modeled as

$$H_{LW, loss} = k_{LW, loss} (273.15 + T_a)^4 \propto k_{LW, loss} T_a, \quad (6)$$

where the power term is approximately linear in T_a for temperature differences < 20 degrees Celsius (see also Mohseni & Stefan, 1999). Finally, the heat input from incoming shortwave radiation, H_{SW} , is a function of sun angle, albedo, and atmospheric effects. Wagner et al. (2011) used the climatologically averaged insolation as a basis function in their T_w model, but most models implicitly assume that $H_{SW} R$ is proportional to T_a (Benyahya et al., 2007).

Combining Equations 3 to 6, and neglecting the evaporation term, we find that H can be linearized as follows:

$$H(t) \approx b_1 T_a + b_2 T_w + b_3 + error, \quad (7)$$

where b_1 , b_2 , and b_3 are constants.

Combining Equation 7 and Equation 2, the heating term can be approximated by:

$$\frac{H}{\rho c_p d} \approx c_1 T_a + c_2 T_w - c_3 Q T_w + c_4 Q T_a + c, \quad (8)$$

Where c is the approximation error and c_1, c_2, c_3 , and c_4 are coefficients. Equation 8 shows that even after many simplifications and approximations, there are still nonlinear interactions between terms such as air temperature and river flow (i.e., the QT_a term). In practice, it is found or assumed that air temperature is the most important factor in heating, and only the T_a dependence is retained (e.g., Erickson & Stefan, 2000, Webb et al., 2003). Most statistical models implicitly start with this assumption, though some non-linear regression approaches have been applied (see review by Benyahya et al., 2007). The discussion above suggests that linear regression models have a basis in the underlying physical dynamics (see also Mohseni & Stefan, 1999). However, a number of assumptions and approximations must be made to represent the 1D-ADE as convert (1) to a linear model form, and a linearized representation of average conditions during a particular season may work less well under unusual or extreme conditions. Simplifying heating to be a linear function of T_a and Q works best during periods of relatively constant water temperature T_w s and river discharge (see also Mohseni & Stefan, 1999). This is one reason why models calibrated to a specific season such as summer often works better than a model fit to an entire year (see below). argu T_a :

Formatted: Not Highlight

For our purposes here, we note that simplifying heating to be a linear function of T_a works best during periods of relatively constant water temperatures and river discharge (see also Mohseni & Stefan, 1999). This is one reason why models calibrated to a specific season such as summer of ten works better than a model fit to an entire year (see below).

The advection term in Equation 1 can similarly be linearized by assuming that either $\frac{\partial T_w}{\partial x}$ or Q is constant or slowly varying, relative to the other. This yields either a regression term in Q or in T_w . Removing When nonlinear terms In summary, the ADE representation of $\frac{\partial T_w}{\partial t}$ in (1) is can be linearized, the following linearized basis function emerges and expressed in terms of three basis functions, T_w , T_a , and Q . (see supplement for more information):

$$\frac{\partial T_w}{\partial t} = b_w T_w + b_a T_a - c_Q Q, \quad (92)$$

where b_w , b_a , and c_Q are coefficients and the minus sign indicates that river flow reduces T_w water temperature. Using the approximation $\frac{\partial T_w}{\partial t} \approx \frac{T_{wn} - T_{wn-1}}{\Delta t}$, we find that T_w at time step n is equal to the T_w at the previous time step ($n-1$), plus a correction that is a function of T_a and Q :

Formatted: Font: Not Italic

$$T_{wn} = T_{wn-1} + \Delta t (b_w T_{wn} + b_a T_a - c_Q Q) \Delta t b_w T_{wn} + \Delta t b_a T_a - \Delta t c_Q Q \quad (103)$$

This Thus, Equations 2 & 3 is depict an autoregressive (AR1) process. Hence, at time $n-1$, T_w is a function of the T_w at time $n-2$, and the T_w at $n-2$ depends on T_w at $n-3$. If we develop and then substitute the solutions for $T_{wn-1}, T_{wn-2}, \dots$ into Equation 103, we find that

$$T_w(t) = \sum_{\tau=0}^{\tau=j} a_{\tau}(t-\tau) T_a(t-\tau) + \sum_{\tau=0}^{\tau=j} b_{\tau}(t-\tau) Q(t-\tau) + C, \quad (114)$$

where a_τ and b_τ are regression coefficients at some time lag τ , C is a constant of regression, and the time period j is chosen to be long enough that the coefficients a_τ and b_τ effectively become negligible and/or statistically insignificant. Further, at the large time lag $\tau = j$, the influence of the time-lagged temperature term in Equation 3 becomes negligible and drops out. The coefficients a_τ and b_τ can be modeled using an exponential filter approach (e.g., Al-Murib et al., 2019); here, as explained below, we estimate the coefficients directly. At a large time lag, the influence of the time-lagged temperature term in Equation 10 becomes negligible and drops out; hence Equation 11 effectively represents T_w as a function of time-lagged T_a and river discharge.

~~Statistical models are often used to interpret and predict T_w patterns, using a number of different regressions, statistical approaches, or machine learning (e.g., Benyahya et al., 2007, Zhu et al., 2018). Within the Pacific Northwest, many studies have developed statistical regression models which use T_a and sometimes also river discharge Q to model measured T_w (Moore 1967; Donato, 2002; Bottom et al., 2011; Mayer, 2012). Such models are simple and run quickly, enabling evaluation of time periods for which in-situ measurements are unavailable and allowing interpretation of primary forcing factors.~~

The discussion above suggests that linear regression models have a basis in the underlying physical dynamics (see also Mohseni & Stefan, 1999). However, a number of assumptions and approximations must be made to represent the 1D ADE as a linear model. Factors such as wind, evaporation, time or spatial variation in parameters and heating terms, and alterations in depth are only approximately represented by T_a and Q . Moreover, depending on conditions, different terms (e.g., depth, heat flux, and velocity) may contribute in varying degrees to the overall heat balance. Thus, a linearized representation of average conditions during a particular season may work less well under unusual or extreme conditions.

2.4 Statistical Model

~~Statistical models are often used to interpret and predict T_w patterns, using a number of different regressions, statistical approaches, or machine learning (e.g., Benyahya et al., 2007, Zhu et al., 2018). Within the Pacific Northwest, many studies have developed statistical regression models which use T_a and sometimes also river discharge Q to model measured T_w (Moore 1967; Donato, 2002; Bottom et al., 2011; Mayer, 2012). Such models are simple and run quickly, enabling evaluation of time periods for which in-situ measurements are unavailable and allowing interpretation of primary forcing factors.~~

We employ a model Willamette River T_w with the by applying a stochastic modeling approach to in eq. (4) (e.g.c.f., Caissie et al., 1998; Benyahya et al., 2007) to the linearized ADE (Equation 4). In this approach, in which the dependent variable (water temperature T_w) and the independent variables (air temperature T_a and river discharge Q) are decomposed into a long term climatological average and a time varying component. A similar approach has also been applied to the Columbia River (Scott, 2020, Scott et al., 2023; Scott et al., 2022); other statistical models applied to this region include Moore (1967), Donato (2002), Bottom et al. (2011) and Mayer (2012).

616 For a generic variable $X(t)$ measured daily, ~~the we define the climatological average is defined~~
 617 as;

$$618 \quad \overline{X(t)} = \frac{1}{y_2 - y_1 + 1} \int_{y_1}^{y_2} \int_{-T/2}^{T/2} X(t) dt dy, \quad (542)$$

619 where $T = 30$ days, t is the integer number of days since the start of the year, y_1 is the beginning
 620 year of the time series (e.g., 1881), y_2 is the end year (e.g., 1890), and the overbar represents the
 621 climatological average. ~~The number of years in the average should be long enough to capture~~
 622 ~~natural variability, but short enough to be statistically stationary (i.e., not overly influenced by~~
 623 ~~land use changes or climate change).~~ The 95% uncertainty in the climatological average is given
 624 by $\frac{t_* \sigma}{\sqrt{N}}$, where $t_* = 1.96$ for a large sample size N , and σ is the standard deviation. In practice,
 625 the number of years we used to define the climatological average is limited by available data.

626 The deviation from climatology, caused for example by a heat wave, is defined as:

$$627 \quad X'(t) = X(t) - \overline{X(t)} \quad (643)$$

628 ~~The climatological average for water temperature, $\overline{T_w(t)}$, is a good first approximation for condi-~~
 629 ~~tions at any given year day, and correctly estimates daily T_w in Portland to within a root mean-~~
 630 ~~square error (RMSE) of ~ 1.5 to 2°C .~~ For a model to have predictive and explanatory power, it
 631 must exhibit a ~~root mean square error (RMSE)~~ ~~less significantly less than $X'(t)$ their climato-~~
 632 ~~logical average.~~ Present day numerical models typically fulfill this criterion and have an RMSE
 633 $< 1^\circ\text{C}$ (Dugdale et al., 2017). ~~Substituting Equation 5 & 6 into Equation 4, our basis~~
 634 ~~To obtain comparable error statistics, we rewrite Equation 11 in terms of deviations of T_w from climatol-~~
 635 ~~ogy, and form the following basis function becomes:~~

$$636 \quad T_w'(t) = \sum_{\tau=0}^{\tau=j} a_\tau(t - \tau) T_a'(t - \tau) + \sum_{\tau=0}^{\tau=j} b_\tau(t - \tau) Q'(t - \tau) + C, \quad (447)$$

637 where the prime indicates a deviation from climatology and other terms are as defined in Equa-
 638 tion 44. Based on experimentation, we use daily T_a' ~~out-lags up~~ to two weeks. Thereafter, we
 639 use average T_a' , to obtain a statistically significant correlation. A 15 day average is used for day
 640 15–30, and 30 day averages are used thereafter, up to 6 months. Similarly, river discharge Q' is
 641 averaged using a 10 day average for day 1–10, a 20 day average for day 11–30, and – a 30 day
 642 average thereafter.

643 A total of ~~8.7~~ statistical models are developed ~~using the basis function infrom Equation 7, using-~~
 644 ~~based on~~ data from the 19th century (1881–1890), mid-20th century (1941–1952), and modern
 645 period (2000–2015) (see Table 2). ~~The models differ in the location of air temperature data and~~
 646 ~~time period used for calibration, and the period modeled.~~ These ~~three calibration~~ periods were
 647 chosen based on available data; they approximate (nearly) pre-development conditions, pre-flood
 648 control conditions, and modern conditions. ~~The models are named based on the first year of cali-~~
 649 ~~bration data and the first letter of the meteorological station used; for example, 1941V and~~
 650 ~~1941D are models trained with 1941–1952 data from Vancouver and Downtown Portland, re-~~
 651 ~~spectively (Table 2).~~ Within each model, we further ~~divide the year into developed~~ a summer
 652 sub-model (July–September), a winter sub-model (January–March) and an annual model, based
 653 on all available data. Experimentation was used to obtain the optimal ~~timespan of~~ winter and

Formatted: Font: Italic

Formatted: Font: Italic

Formatted: Not Highlight

summer models, and the annual model is used for months not covered by the winter or summer models. For example, including June or October into the summer model significantly reduced the goodness of fit for the summer model was found for covers July to September, and the statistical influence of river discharge, consistent with the observation that the horizontal temperature gradient is largest during this period from July to September (Figure 2b). Through experimentation, we also determined that discharge only produces a statistically significant effect for summertime models based on 1941–1952 and 2000–2015 data (i.e., not winter or annual models). This result is consistent with previous studies (e.g., Isaak et al., 2012) and with estimates of $\frac{\partial T_w}{\partial Q}$ (section 2.3, Figure 2) which suggests that discharge effects are most prominent in summer.

Results show that the best-fit coefficients generally decrease in magnitude as T_w (Figure 3a,b,c) and river discharge (Figure 3d) are lagged backwards in time. Further, the decorrelation structure is different for the 19th, mid 20th, and 21st century models (Figure 3); hence, for the same forcing, these statistical models will produce a different output. Statistically significant coefficients are found at up to 3 month lag in the 1880s model, and 4 months in the others.

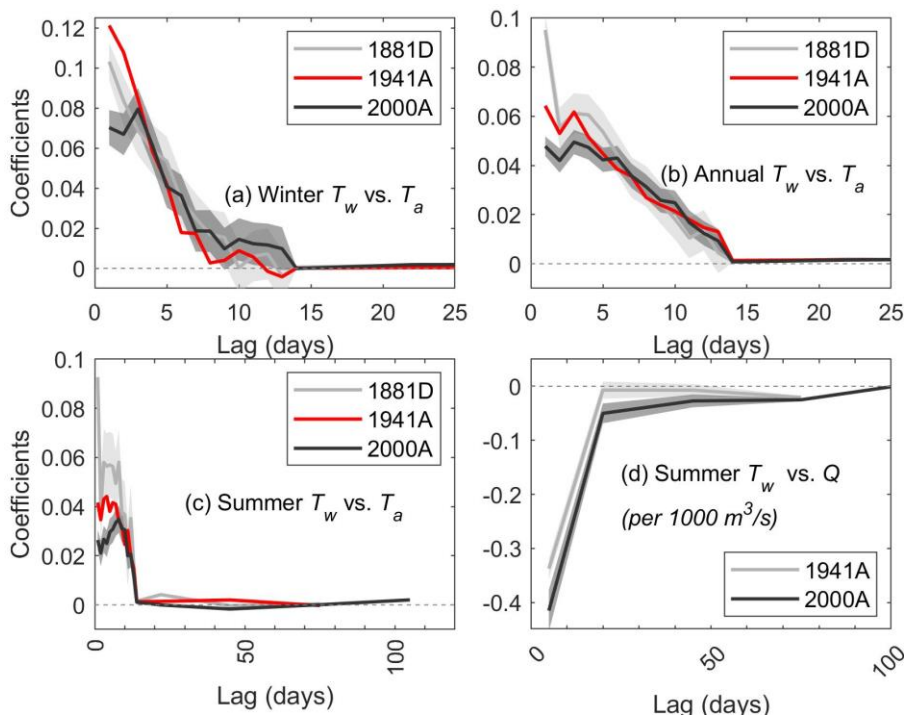


Figure 3: Coefficients for statistical model vs time lag for (a) air temperature (T_a) in the winter model (Nov–Mar); (b) T_a in the annual model (all months); (c) T_a in the summer model (July–Sept) and (d) discharge Q in the summer model (July–Sept). The 1881 model is calibrated to 1881–1890 T_w data, the 1941 model is calibrated to 1941–1952 T_w data, and the 2000 model is calibrated to 2000–2015 T_w .

674 ~~data. The letter denotes whether T_a data was sourced from Downtown Portland (D) or from the Airport~~
 675 ~~(A). Similar results are found for the model based on Vancouver air temperature data (not shown). No~~
 676 ~~statistically significant effect of river discharge was found for winter or annual models, and the 1990s~~
 677 ~~summer model, and are not shown.~~

678 Each statistical model produces an estimate of T_w over the period of record of its underlying T_o
 679 record (Table 2; data available as supplemental information). Based on ~~these output~~ time series,
 680 a composite estimate of modeled T_w was produced using the best available statistical model. A
 681 compromise was required when deciding which era of model to use in the composite, since be-
 682 cause there is no clear absolute delineation between pre- and post-reservoir conditions, or be-
 683 tween a nearly natural and substantially altered landscape. Models based on Vancouver T_a air
 684 temperature measurements were used pre-1868, Eola T_a measurements from 1870–1874, down-
 685 town Portland from 1874 to –1939, and the Portland Airport data thereafter. For each year, the
 686 two seasonal sub-models were used, with the annual sub-model used at other times. The mid-
 687 20th century calibration, representing pre-reservoir, post-landscape change conditions, was ap-
 688 plied to the 1900–1960 period (1941A model); thereafter, we assume modern flood control, and
 689 applied the modern calibration (2000A model). Estimates from 1869–1899 Pre 1900 estimates
 690 used the calibration based on 1880s T_w water temperature data (1881D model). T_a No overlap oc-
 691 curring between Vancouver T_a and Willamette T_w measurements during the 19th century. Hence,
 692 pre-1868 estimates used the mid-20th century calibration to Vancouver T_a (the 1941V model),
 693 since a 19th century calibration was unavailable. data, as follows.

694 First, for each station, estimates from the two seasonal sub-models were combined, with annual
 695 sub-model results used at other times. To avoid (typically small) discontinuities between sub-
 696 models, a 15-day linear relaxation period between sub-model start and stop times was applied.
 697 Next, a composite estimate for T_w was made for the 1850–2020 period, using the best available
 698 meteorological measurements and statistical models. Vancouver measurements were used pre-
 699 1868, downtown Portland from 1874 to 1939, and the Portland Airport data thereafter. Water
 700 temperature estimated from Eola T_a measurements were used to fill the 1870–1874 period. A
 701 compromise was required when deciding which era of model to use in the composite, since there
 702 is no clear delineation between pre and post reservoir conditions, or between a nearly natural and
 703 substantially altered landscape. The mid-20th century calibration, representing pre reservoir,
 704 post landscape change conditions, was applied to the 1900–1960 period; thereafter, we assume
 705 modern flood control, and applied the modern calibration. Pre 1900 estimates used the calibra-
 706 tion based on 1880s data, except for the Vancouver period (1850–1868), which used the mid-
 707 20th century model because there was no 19th century model. The validity of the composite mod-
 708 eled T_w is assessed, to the extent possible, through comparison with in-situ measurements (see
 709 Results).

710 ~~Uncertainty~~ The skill of each statistical model was assessed by evaluating the root-mean-square
 711 error (RMSSME) between the composite model estimate and measurements. Our values are
 712 compared against, and comparing against the RMSE found between measurements and using
 713 eclimatology. The uncertainty in each of modeled temperature estimates was assessed using a
 714 Monte Carlo approach. Two thousand possible ensembles of the model coefficients were created,
 715 under the assumption that coefficient uncertainty (obtained by the linear regression) was nor-
 716 mally distributed. The 95th percentile of the resulting spread of solutions is reported.

Formatted: Font: Italic

Formatted: Font: Italic, Subscript

Formatted: Font: Italic

Formatted: Font: Italic, Subscript

Formatted: Font: Italic

Formatted: Superscript

Formatted: Superscript

Formatted: Space After: 24 pt

2.5 Attribution Analysis

We approximate the influence of changing air temperatures, changing river discharge, and the integrated effect of river system changes through experimentation using our statistical models. The following first-order effects are approximated:

1. Climate change impacts: Climate change has driven changes in the 30 year average climatology of daily air temperature in the region (e.g., Mote et al., 2019). We estimate the influence of changed air temperature climatology by running our modern statistical model (model 2000A; see Table 2) using historical downtown climatology (1875-1904) and modern Portland airport climatology (1991-2020) (daily time scale). River flow is kept constant and does not influence results. The difference between these scenarios is attributed to climate change. The uncertainty in modeled T_w is assessed by perturbing input climatology with plausible uncertainty and bias estimates in T_a .
2. Effect of altered river flow: Changes in river flow seasonality, caused primarily by water resources management but also influenced by changing snow pack (e.g., Naik & Jay, 2011) can influence water temperatures in our 1941 and 2000 era summer models (Table 2; river flow was not statistically significant in 1881 era models). The change in the river hydrograph (see Figure 2a) is applied to the 1941 and 2000 era models (Table 2), with the T_a input kept the same between models. The difference in model output shows the influence of altered average river flow on modeled T_w for the July-September time frame between pre-reservoir (1901–1940) and modern (1981–2020) conditions.
3. Integrated system changes: Over the past 150 years, multiple landscape and watershed changes, including loss of riparian habitat and reservoir construction, have occurred (Section 2.1). We investigate their net influence on T_w by applying the same river flow and T_a data from 2000–2020 to models from different eras (Table 2). Because the input into each statistical model is identical, any differences in output T_w are caused by changes in model coefficients (Equation 7). The uncertainty analysis in section 2.4 is applied to determine whether differences are statistically significant, consistent with the hypothesis that river system changes have altered the river's response to external heating and other forcing.

Formatted: List Paragraph, Numbered + Level: 1 + Numbering Style: 1, 2, 3, ... + Start at: 1 + Alignment: Left + Aligned at: 0.25" + Indent at: 0.5"

Formatted: Font: Italic

Formatted: Font: Italic, Subscript

Formatted: Not Highlight

Formatted: Subscript

Formatted: Font: Not Italic

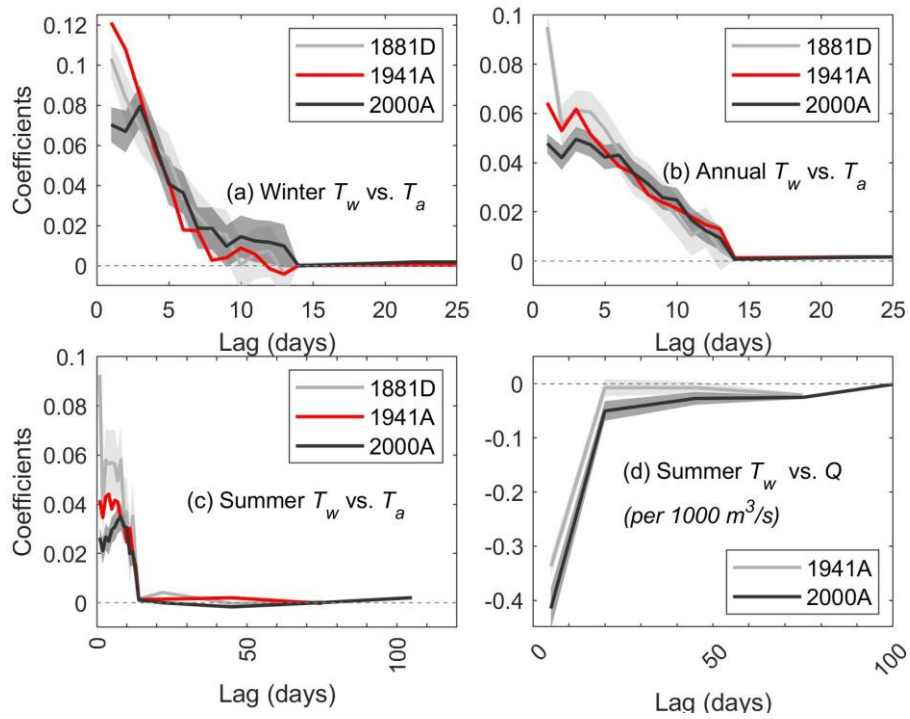
Formatted: List Paragraph, Space After: 24 pt, Numbered + Level: 1 + Numbering Style: 1, 2, 3, ... + Start at: 1 + Alignment: Left + Aligned at: 0.25" + Indent at: 0.5"

3.0 Results and Discussion

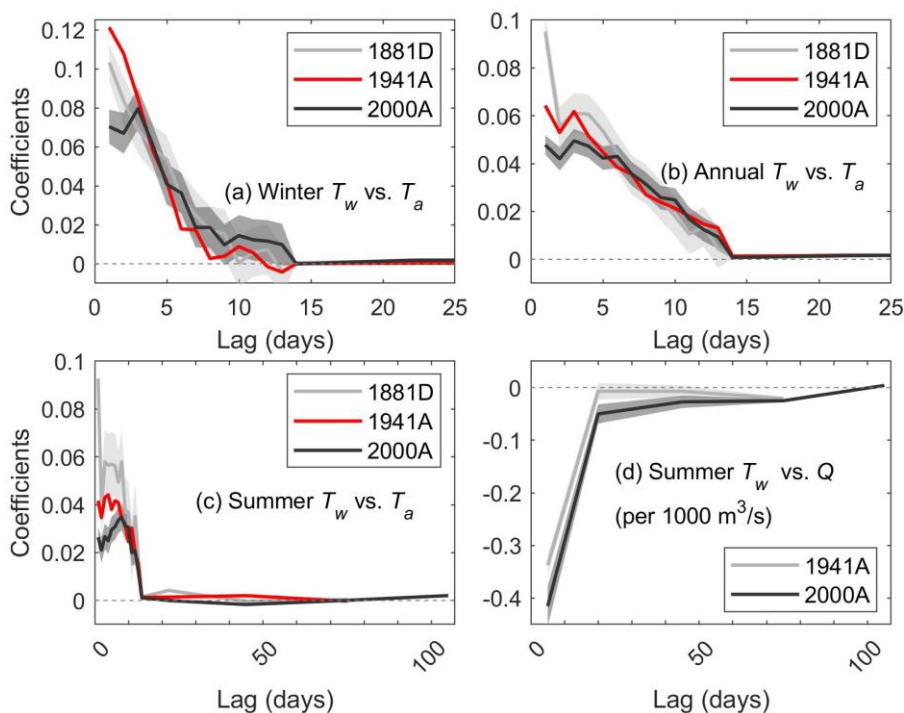
3.1 Model Assessment

Results show that the best-fit coefficients (see Equation 7) generally decrease in magnitude as T_a (Figure 3a,b,c) and river discharge (Figure 3d) are lagged backwards in time. Further, the decorrelation structure is different for the 19th, mid-20th, and 21st century models (Figure 3); hence, for the same forcing, these statistical models will produce a different output (Equation 7). Statistically significant coefficients are found at up to a 3-month lag in the 1880s model, and 4 months in the others. The magnitudes of coefficients at 2–4 month lags are larger today, at ~ 0.0025 $^{\circ}T_w/^{\circ}T_a$ per day (modern) vs. ~ 0.0017 $^{\circ}T_w/^{\circ}T_a$ per day (1940s; annual model). As discussed later, the changes in the statistical model between eras likely occurs due to the integrated effect of land use and water management changes.

757
758



759



Formatted: Space After: 18 pt, Tab stops: 5", Left

Figure 3: Coefficients for statistical model vs time lag for (a) T_w in the winter model (Nov–Mar); (b) T_w in the annual model (all months); (c) T_w in the summer model (July–Sept) and (d) discharge Q in the summer model (July–Sept). The 1881 model is calibrated to 1881–1890 T_w data, the 1941 model is calibrated to 1941–1952 T_w data, and the 2000 model is calibrated to 2000–2015 T_w data. The letter denotes whether T_w data was sourced from Downtown Portland (D) or from the Airport (A). Similar results are found for the model based on Vancouver T_w air temperature data (not shown). No statistically significant effect of river discharge was found for winter or annual models, and the 1880s summer model, and are not shown.

Formatted: Not Highlight

Time-series comparisons of modeled and observed T_w water temperature (Figure 4) and statistical evaluations (Table 2) confirm that the statistical-stochastic model reproduces reasonably well year-to-year differences in T_w and weekly–monthly perturbations caused by persistent warm/cold weather. Some synoptic scale events of less than a week are only partially captured, possibly because of factors not included in the model: e.g., (such as) cloud cover, wind, or depth changes due to backwater from the Columbia River; (see also Wagner et al., 2011), and the tendency of statistical models to underestimate extremes. The RMSE between the measured and modeled daily minimum T_w varies from 0.87 to 1.1 °C for the annual model, with RMSE as low as 0.53 °C and 0.72 °C for the summertime and wintertime models, respectively (Table 2). Results are less good using Eola (1870–1892), a historical weather station which is was located

~70km from Portland and may imperfectly represent local meteorological forcing. ~~On a~~For monthly averaged ~~estimates~~scale, RMSE varies from ~0.3 to 0.9 °C, with the best agreement obtained during the modern period and the summertime sub-models (Table 2).

Our statistical model results compare favorably with numerical models, other statistical approaches, and climatology. For example, the RMSE at Portland for a calibrated numerical model based on measurements from April ~~through~~ September 2002 was 0.43 °C (Berger et al., 2004), compared to 0.52 °C for our model over the same period. Similarly, ~~the our~~ models performs significantly better than estimates based on T_w climatology, which we calculate ~~has have~~ a root-mean-square error (RMSE) of 1.86, 1.46, and 1.43 °C for the 1881–1890, 1941–1952, and 2000–2015 calibration periods, respectively (see Table 2). Our results compare well with traditional linear regression and stochastic models, which have reported RMSE of ~0.6–1.9 °C, depending on model type, river size and location, and averaging period (e.g., Caissie 1998; see also review by Benyahya et al., 2007 and references therein). More recent statistical models, including air2stream (Toffolon and Piccolroaz, 2015) and machine learning approaches (e.g., Fiegl et al., 2021), report RMSE of 0.5–1 °C on a daily scale, similar to the results presented here (Table 2). Results are also comparable to numerical models that generally have an RMSE <1 °C (e.g., Dugdale et al., 2017). We conclude that ~~the our~~ statistical models accurately represents the most important factors affecting T_w , as long as the underlying measurements driving the model are reasonably accurate and representative of local conditions.

Modeled T_w estimates based on models using different T_a data series (Table 2) ~~compare well~~ with each other, with similar averages and variability. During their period of overlap from 1940–1973, daily modeled T_w values~~water temperatures~~ are slightly larger (0.08 °C) using the airport model (1941A) than the downtown Portland model (1941D). Similarly, the Vancouver model (1941V model) is 0.02 °C lower than the airport model (1941A) between 1940 and 1965. For the same periods, the daily RMSE between the 1941A model T_w and the 1941D and 1941V models is 0.29 °C and 0.32 °C, respectively. For the 1896–1965 period, the 1941D and 1941V models show a mean difference of 0.06 °C (Vancouver larger), and an RMSE of 0.37 °C. ~~These observations provide an order of magnitude estimate of the aggregate influence of input data and model variability on uncertainty, whether caused by spatial variations in T_a , differences in the statistical coefficients, or or instrumental measurement precision uncertainty or bias errors (presumably or is another source of uncertainty).~~ The consistency and small RMSE between model results improves our confidence in both the input data and the results.

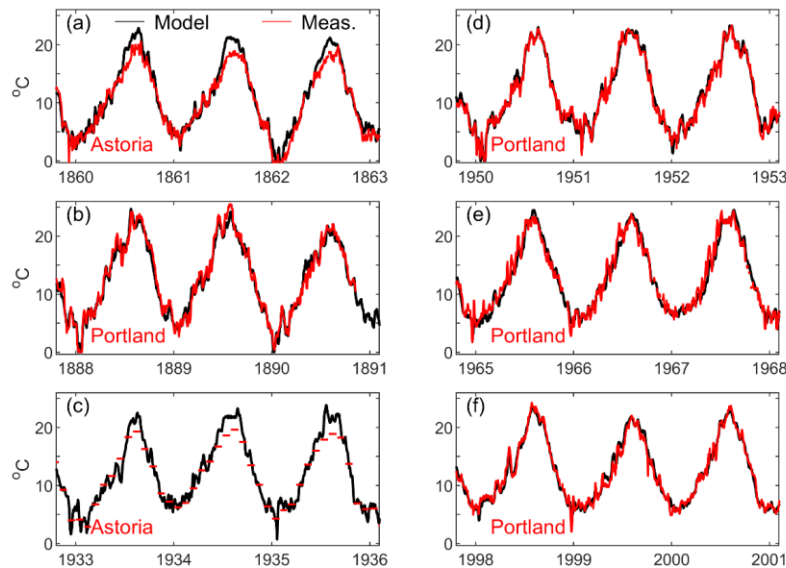


Figure 4: Comparison of modeled and measured T_w for six three-year periods of three years. The composite Portland T_w is used in (b), (d), (e) and (f), while Astoria measurements are used in (a) and (c). Only monthly averages of T_w are available at Astoria from 1925 to 1940 and 1943–1948 (see Table 1). Black is modeled, red is measured.

One of the factors driving the larger RMSE in the historical model is the larger overall system variance measured for 19th century T_w . The typical distribution of T_a anomalies from the climatological mean has remained stationary between different time periods, and the standard deviation is nearly the same (within ~5%; Figure 5). However, between the 1880s and the 2000–2015 period used for calibration, the distribution of measured T_w anomalies markedly contracted—, and the standard deviation decreased from 1.86 to 1.42 °C (Figure 5). Since the distribution of T_a anomalies remained similar, a likely explanation for the decreased variance in T_w is anthropogenic change to the local environment (e.g., flow regulation, landscape changes, system-channel deepening), namely simplification of the riverscape (Peipoch et al. 2015) (see discussion), rather than changes in meteorological forcing (see below for further discussion).

Formatted: Superscript

Formatted: Not Highlight

Formatted: Highlight

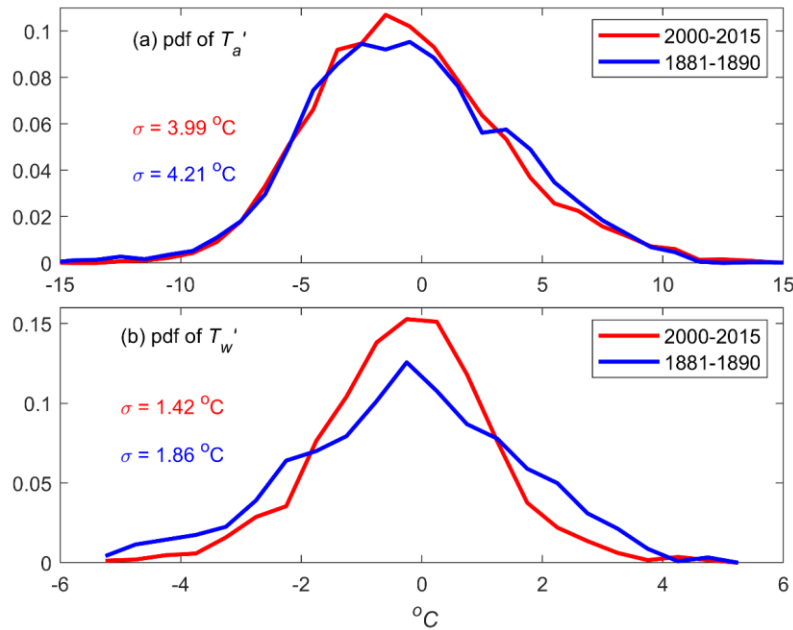


Figure 5: The measured probability distribution density function (pdf) and standard deviation σ of T_a and T_w anomalies around the 30d climatological mean for the 1881–1890 and 2000–2015 periods. The anomalies (T_a' and T_w') are defined as the deviation from the 30 day climatological mean (see Equation 5 & 6). The y-axis gives the probability density.

3.2 Water Temperature Changes in lower Willamette

Model results and measurements show that water temperatures have increased steadily since the 1800s. Increases are observed at all times of the year (Figure 6), leading to an increase in annually averaged T_w of 1.1 ± 0.2 °C/century (Figure 7). The largest increase occurred in winter; during January–February, the trend in average T_w is 1.3 ± 0.3 °C/century (Figure 6a). Similarly, the minimum annual temperature is increasing quickly, at 1.8 ± 0.5 °C/century (Figure 7b). The smallest bi-monthly averaged trends occur in late spring, during May–June (0.82 ± 0.3 °C/century trend; Figure 6d). Maximum summer temperatures are trending upwards at $\sim 0.9 \pm 0.3$ °C/century (Figure 7c), smaller than the annual average. Overall, model results (grey) track available in-situ measurements (red) well, except for some months during periods of lesser data quality in the 1960s–1970s (Figure 6 & 7). Therefore, consistency of modeled and measured trends further increases confidence in our results.

Formatted: Font: (Default) Times New Roman, 12 pt

Formatted: Font: (Default) Times New Roman, 12 pt

Formatted: Space After: 24 pt

Formatted: Font: (Default) Times New Roman, 12 pt

Formatted: Font: (Default) Times New Roman, 12 pt

Formatted: Font: (Default) Times New Roman, 12 pt

Formatted: Font: (Default) Times New Roman, 12 pt

Formatted: Subscript

Formatted: Subscript

Formatted: Font: (Default) Times New Roman, 12 pt

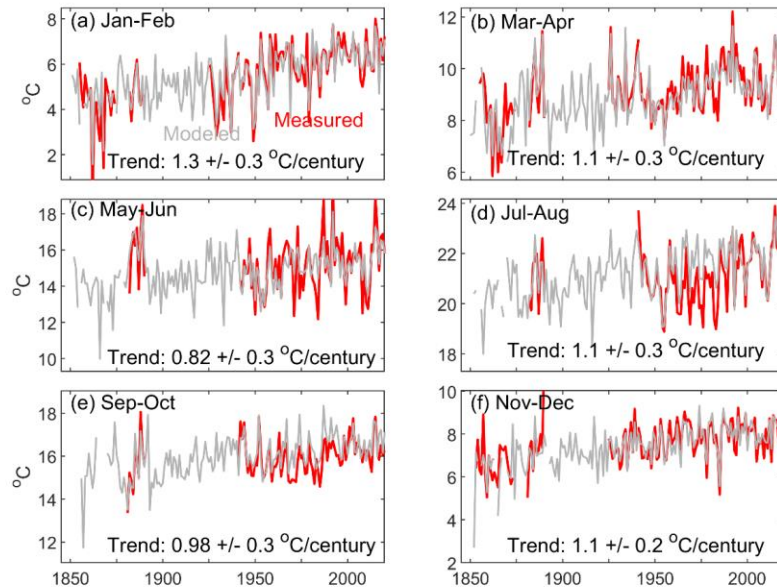


Figure 6: Seasonal trends in water level, averaged over two-month water periods. A correlation is found between measurements (red) and model results (grey) are correlated. The trends and 95% confidence interval are based on a linear regression to model results, 1850–2020. November–April data from 1854–1876 are from Astoria, Oregon (see Talke et al., 2020). Note different limits on the y-axis scales.

No single event or individual system perturbation appears to be causing trends, as there are no step-function changes or inflection points in T_w trends (Figures 6 & 7). Instead, an upwards tendency in T_w is interspersed-punctuated by large year-to-year variability. In the modern system, the largest interannual variation occurs during the typically high-flow the spring-period (May–June), with swings of $\sim 5^\circ\text{C}$ observed in bimonthly averages between years (Figure 6). The typically low-flow late summer and autumn season (September–December) is least variable (order $\pm 2^\circ\text{C}$ variability between years). Historically During the 19th century, greater year-to-year fluctuations occurred in both measurements and model means results during all seasons, typically $4\text{--}6^\circ\text{C}$ (Figure 6). The largest decreases in year-to-year variability are observed, particularly during the cooler half of the year between September to February (November–April). Cool-season measurements at Astoria (1854–1876) from November–April between November and April confirm this variability, and track modeled results despite its location on the Columbia River (see e.g. Figure 4a and 4c, Figure 6). The correspondence likely occurs because during late fall and winter, proportionally more water in the lower Columbia is sourced from coastal tributaries, especially the Willamette River, than during other times of year (see Naik and Jay, 2011 and Hudson et al., 2017).

Formatted: Superscript

Both climatic factors and system changes drive the reduction in interannual variability in T_w . Storage reservoirs, with a large thermal inertia, are one factor (see section 3.3). The change from a multi-braided, shallow channels to a single, deeper channel is also likely influential. Another reason for historical T_w variability in winter was the occasional occurrence of deep freezes that no longer occur. During the winters of 1861–62 and 1867–1868 winters, for example, $T_{a,air}$ temperatures remained below 0 °C for 32 and 31 days, respectively, and newspapers recorded ice skating on the lower Willamette River. Navigation in Portland Harbor was halted or hindered by ice from New Year's Day until mid-March, 1862. No 20th-century winter matched the duration or severity of these events, though 18–19 freezing days (maximum below 0 °C) were recorded in 1915–1916, 1929–1930, and 1949–1950. In 1979, air temperatures remained below 0 °C for a total of 14 days; since 1980, no winter has produced more than 9 sub-freezing days. Because However, some historical winters were mild (e.g., only one freezing day was recorded in 1862–1863), and historical water temperatures in winter T_w were much more variable than today.

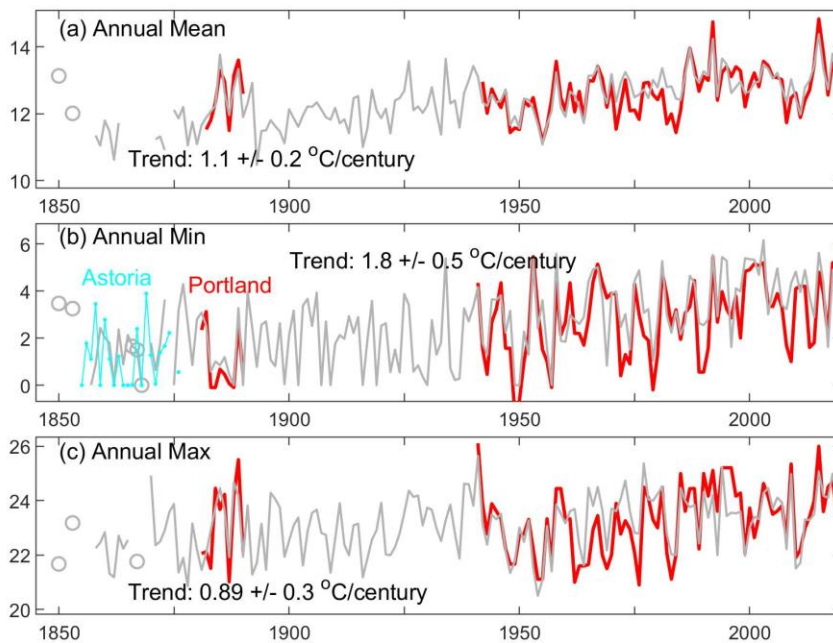


Figure 7: Time rate of change of annual mean, annual minimum, and annual maximum T_w . Grey denotes model data, red denotes data from Portland region, and cyan denotes T_w measurements in Astoria (annual minimum only, [panel b](#)). The trend is calculated by regression fit to [model results over the 1850–2015](#) period. Evaluation is based on daily minimum T_w (see section 2). Years in the 1850s and 1860s without sufficient model data are excluded.

Results suggest that T_w has ~~always~~ exceeded a threshold of 20 °C during summer for ~~~15–90~~ days ~~between for the entire 1850–present~~ ~~2015–21~~, even during the 1800s period (Figures 4, 7c, 8 and 9), ~~despite generally cooler 19th century conditions~~. A spaghetti plot of all available in-situ data shows that ~~maximum T_w and most T_w measurements exceed exceedances of the 20 °C T_w threshold~~ ~~have occurred~~ in July and August (Figure 8). ~~Peak temperatures typically occur during July or August, with no secular trend in timing observed (Figure 8, 9). The timing meteorological heat waves within a summer—which appears to be random—drives the timing of the peak.~~ During some cool summers historically (e.g., 1949; see Figure 8), ~~T_w temperatures sometimes temporarily dipped below~~ ~~oscillated around and near~~ 20 °C during summer, ~~and remained above the threshold for less than 2 months~~. In other years, ~~T_w it~~ reaches a peak of 25–26 °C, ~~and water temperatures~~ and remains above the ~~biologically important~~ 20 °C threshold from June to September (Figures 8 & 9). During the hot, low river-discharge summers of 1889 and 2015 (Figure 8), ~~water temperature T_w s~~ exceeded 20 °C for 91 and 95 days, respectively. ~~The biggest difference between the two years, in line~~ ~~consistent~~ with other observations, is that T_w was more variable during the summer of 1889 than in 2015.

Formatted: Superscript

Formatted: Font: Not Italic

Formatted: Font: Not Italic

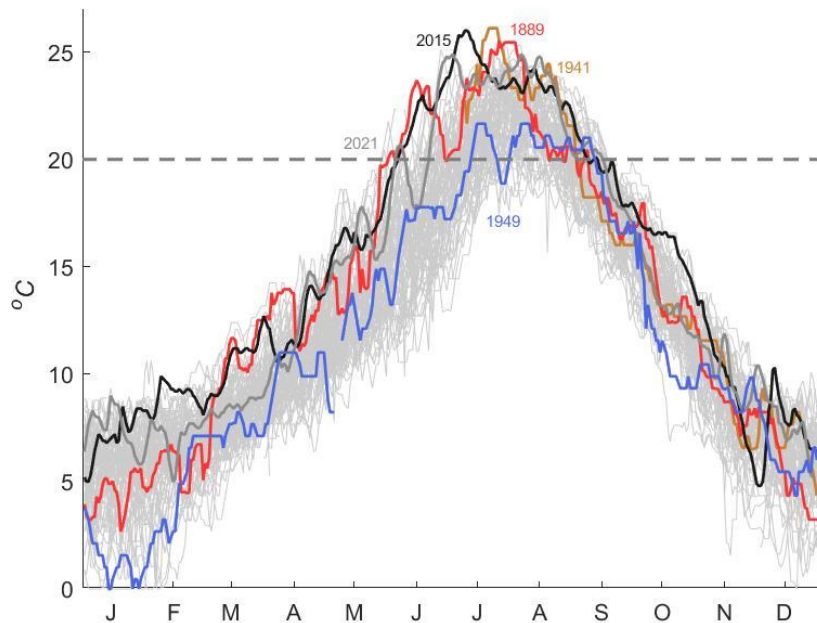


Figure 8: Spaghetti plot of all measured T_w data from between 1881–1890 and 1941–2021. Five years (1889, 1941, 1949, 2015, and 2021) are colored as labeled for comparison. The tick marks on the x-axis denote the middle of each month. Time is labeled at the midpoint of each month.

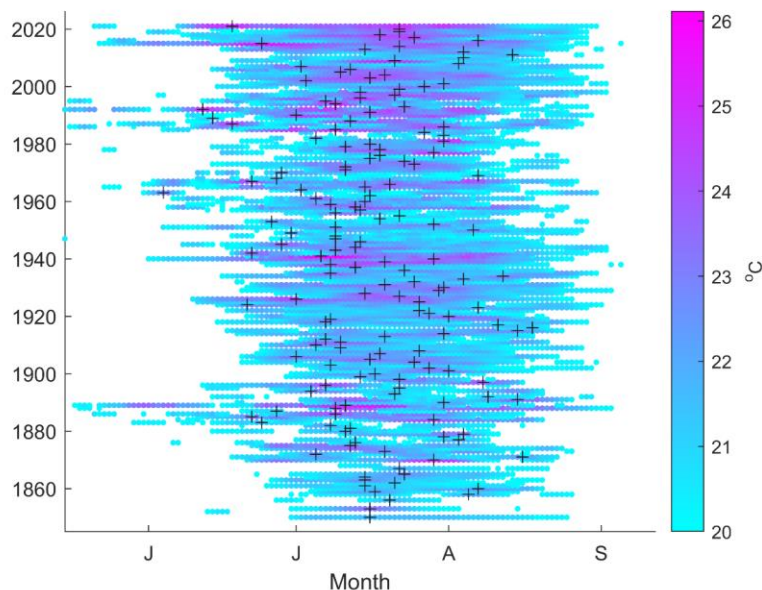


Figure 9: Summertime *Willamette River* T_w values in the Willamette River that exceed a threshold exceedances of 20 °C, from 1850 to 2021. The instrumental record is used between 1881 and 1890 and 1941 to 2021, and the remainder is infilled with modeled T_w . Crosses denote the time of the peak annual T_w . Missing T_a air temperature data precluded peak estimates for 1851–1852, 1854–1855, 1857, 1866, and 1868–1869 (see supplemental data). The tick marks on the x-axis denote the middle of each month. Time is labeled at the midpoint of each month on the x-axis.

Summers with persistently elevated water temperature T_w s occur more often today than historically, even though warm waters occurred in some historical years (Figures 8 & 9). On average, T_w water temperatures are above the 20 °C threshold earlier in the season and exits later than in the 1800s (Figure 9). Between 1881–1890, measurements show that the 7-day average temperature exceeded the effective regulatory limit of 20.3 °C (see Introduction a 0.3 °C allowance is added to the 20 °C limit; see OR-DEQ, 2006) between 11–80 days, with an average of 42 days, with a range of 11–80 days. For the 2000–2021 period, the range was 35–92 days of exceedances, with an average of 63 days (2 months) (see also Figure 9). Thus, there is both an increased number of exceedances and a decreased (though still substantial) year-to-year variability. The more consistently warm summer water temperatures help explain the observed upward trend in T_w (Figure 7). Interannual variability has also decreased, due in part to decreased sensitivity to synoptic (weather) related changes. Evaluated using a 10-year average, the number of days per year that exceed 20 °C increased by roughly ~50% (20d) between 1850 and 2020, from around 40 d yr⁻¹ to more than 60 d yr⁻¹ (Figure 10), an increase of ~20 d. The threshold of 22 °C was exceeded relatively rarely in the 1800s (<5 days per year), but is now exceeded nearly

40 days per year. Before about 1960, there was more variability T_w values with and T_w exceedances

between decades than at present.

The number of cold-water days in winter has declined precipitously as overall temperatures have warmed (Figure 10a). Water temperatures are now rarely below 4 °C, compared to about 25 d

Formatted: Highlight

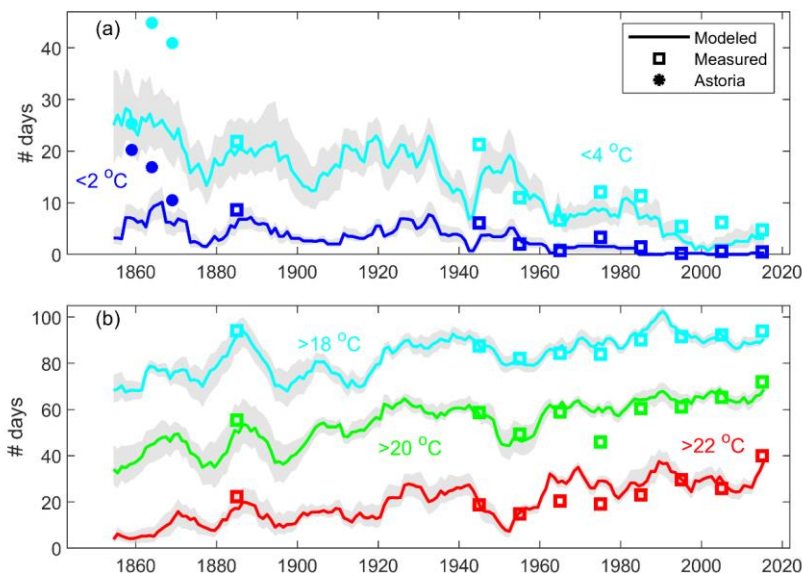


Figure 10: Comparison of the modeled and measured number of days per year from 1850 to 2020 that T_w is (a) below thresholds of 2°C and 4°C and (b) above thresholds of 18°C, 20°C, and 22°C. Square symbols denote the 10-year average based on measurements, while the solid line is a running 10-year average of modeled T_w . Measurements based primarily on bias-corrected upstream gauges (1962, 1983–1984) are excluded. Grey shading is the 95% confidence interval, based on resampling of model coefficients using a Monte-Carlo based technique. Wintertime measurements from Astoria (1854–1876) are included in (a) for comparison.

The number of cold-water days in winter has declined as overall temperatures have warmed (Figure 10a). Water temperature T_w is now rarely below 4 °C, compared to about 25 d per year in the mid-1800s. Similarly, near freezing temperatures (below 2 °C) were common in the 1800s (up to 10 d yr⁻¹), but almost never occur now. While an increase in winter T_w water temperatures has received much less attention than summer time trends, this shift is also ecologically important (e.g., Webb & Weber, 1993; Caissie, 2006). For example, cold water events and winter

time conditions influence the survivability and recruitment of fish by altering their biotic interactions, habitat use, physical condition, feeding rates, and community structure (see reviews by Hurst 2007; Brown et al., 2011; Weber et al., 2013). It is also possible that historical wintertime conditions, such as the deep freezes discussed above, provided some protection against non-native plants and fauna that thrive in warmer waters.

3.3 Interpretation of water temperature changes

In general, seasonal patterns of measured T_w and shifts between 19th and 21st century data are consistent with measurements of T_a , with some slight variations in timing and magnitude (Figure 11). Measurements in Portland indicate that the daily maximum ~~air temperatures (T_a)~~ increased by 1.3 °C between the 1875–1904 and 1991–2020 periods (Figure 11b), consistent with warming trends of 0.5–2 °C per century at 100+ stations throughout the Pacific Northwest (Mote et al., 2003). ~~and an average increase of 1.1 °C since 1900 (Mote et al., 2019).~~ The smallest increases in Portland T_a occur in spring (April–June) and in late fall (November–December), and the largest occur in January–February and July–October, again consistent with T_a trends in the Maritime Pacific Northwest (Mote, 2003). We find little evidence that the heat-island effect (e.g., Voelkel et al., 2018) is substantially affecting our these trends (see supplemental information). Regional data processed for inferred biases suggest a slightly smaller average change of 0.9 °C over a similar period (see Scott et al., 2023), and overall the Pacific Northwest increased by 1.1 °C since 1900 (Mote et al., 2023). Interestingly, the 1880s was an anomalously warm decade for both $T_{a,air}$ and water temperature T_w measurements; thus, $T_{a,air}$ temperature climatology over a 30y period shows a greater change between the 19th century and present-day (Figure 11a, 11b) than the shorter periods of T_w water temperature available for calibration (Figure 11c, 11d); see supplemental information for additional discussion).

Formatted: Space After: 18 pt

Formatted: Superscript

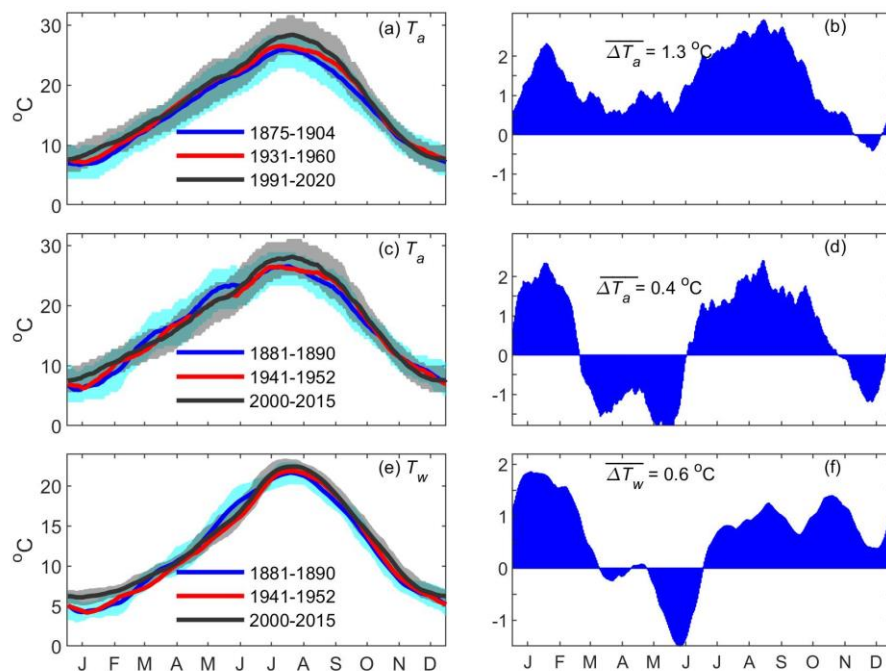


Figure 11: T_a and T_w climatology in Portland (a,c,e) and the corresponding difference between the modern (1991–2020) and historical (1881–1890) periods (1881–1890) in for T_a (b,d,e) and T_w (f). The T_a difference plot in (b) and (d) is the difference between late 19th and early 21st century air temperature data in (a) and (c), respectively. The difference in (f) is the difference between 2000–2015 and 1881–1890 T_w data. Climatology is determined using a 30d moving average; shading denotes the 25th and 75th percentile of the measurements. A 30-year average is used in (a); the time periods for (c) and (e) are determined by the time period used to calibrate the T_w model. The tick marks on the x-axis denote the middle of each month. The average T_w difference between the modern and earliest period is provided in (b,d,e).

Within Portland, the large summertime increase may be influenced by the urban heat Island effect (e.g., Voelkel et al., 2018). However, the city has been relatively urbanized (cleared of forest) since the beginning of the time series, and T_a measurements have primarily occurred by either the Willamette or Columbia River, both reasons that changes in temperature bias caused by infrastructure may be relatively small. Moreover, the distribution of air temperatures around the climatological mean has remained virtually unchanged (Figure 5). Given the long history of Portland and later the Airport as the primary regional measurement station, and the consistency of trends with the regional average (e.g., Mote et al., 2019), we conclude that the T_a measurements are reasonably representative of regional climate patterns.

Formatted: Font: (Default) Times New Roman, 12 pt

Formatted: Font: (Default) Times New Roman, 12 pt, Superscript

Formatted: Font: (Default) Times New Roman, 12 pt

Formatted: Font: (Default) Times New Roman, 12 pt, Superscript

Formatted: Font: (Default) Times New Roman, 12 pt

Formatted: Font: (Default) Times New Roman, 12 pt, Italic

Formatted: Font: (Default) Times New Roman, 12 pt

Formatted: Font: (Default) Times New Roman, 12 pt

Formatted: Font: (Default) Times New Roman, 12 pt

1090 Average air temperatures during the 1881–1890 calibration period (during the Signal Service T_w
1091 measurements) are only 0.4 °C cooler than the 2000–2015 calibration period (Figure 11d), mark-
1092 edly lower than the 1.3 °C difference between the 30y climatological averages (Figure 11b). A
1093 possible reason is that pre-1888 measurements may not have been properly sheltered (Mote
1094 2003). However, comparison with T_w measurements (compare Figure 11c with 11e) suggests
1095 that air and water temperature patterns during this decade were similar and warmer than previous
1096 and subsequent decades. For example, both springtime T_a and T_w measurements in the 1880s
1097 were higher than instrumental measurements from the 2000–2015 period. The correspondence
1098 between T_a and T_w measurements in the 1880s increases confidence that measurements indicate a
1099 real climate signal, possibly caused by decadal fluctuations in climate (e.g., Peterson & Kinkel,
1000 2001), rather than an instrumental artifact.

1001

1002 3.3 Causes of water temperaturewater temperature changes

1003 3.3.1 Causes of T_w Change

1004

1005 We next ~~approximate-analyze the~~ the magnitude of factors causing T_w change using a series of
1006 sensitivity studies. ~~These experiments that~~ provide an order-of-magnitude assessment of how
1007 sensitive ~~modeled T_w the system is to~~ changed ~~model~~ coefficients or shifts in input data such as
1008 ~~T_a air temperature~~ (see section 2.5). input data. ~~We evaluate three key drivers. First, climate~~
1009 ~~change impacts: The climatological T_a increase since the 19th century in Portland is applied~~
1010 ~~(Figure 11b), while river flow and the statistical model are kept constant.~~

1011

1012 1. ~~Integrated system changes:~~ By applying the same input data to models from different
1013 time periods, we explore how the ~~T_w system response~~ has changed to the same perturbations.
1014 River flow and T_a data from 2000–2020 are used. ~~Second, integrated system changes: By ap-~~
1015 ~~plying the same input data to all models (Table 2), we explore how the T_w response is different~~
1016 ~~between models from different eras. River flow and T_a data from 2000–2020 are used. Because~~
1017 ~~model coefficients are different between eras (Figure 3), the results show the effect of system~~
1018 ~~changes.~~

1019 2. ~~The effects of climate change impacts:~~ The climatological T_a increase since the 19th
1020 century in Portland is applied (Figure 11b), while river flow and the statistical model are kept the
1021 ~~sameconstant. Third, the~~

1022 3. ~~The eEffect of water resources management.~~ The change in the river hydrograph (Fig-
1023 ure 2a) is applied, with the system coefficients and T_a held constant.

1024

Formatted: Font: (Default) Times New Roman, 12 pt

Formatted: Font: 14 pt

Formatted: Normal, No bullets or numbering

Formatted: Font: Not Italic

Formatted: Font: Not Italic, Not Superscript/ Subscript

Formatted: Font: Not Italic

Formatted: No underline

Formatted: No underline

Formatted: Font: Not Italic

Formatted: Font: Not Italic

Formatted: Font: Not Italic, Not Superscript/ Subscript

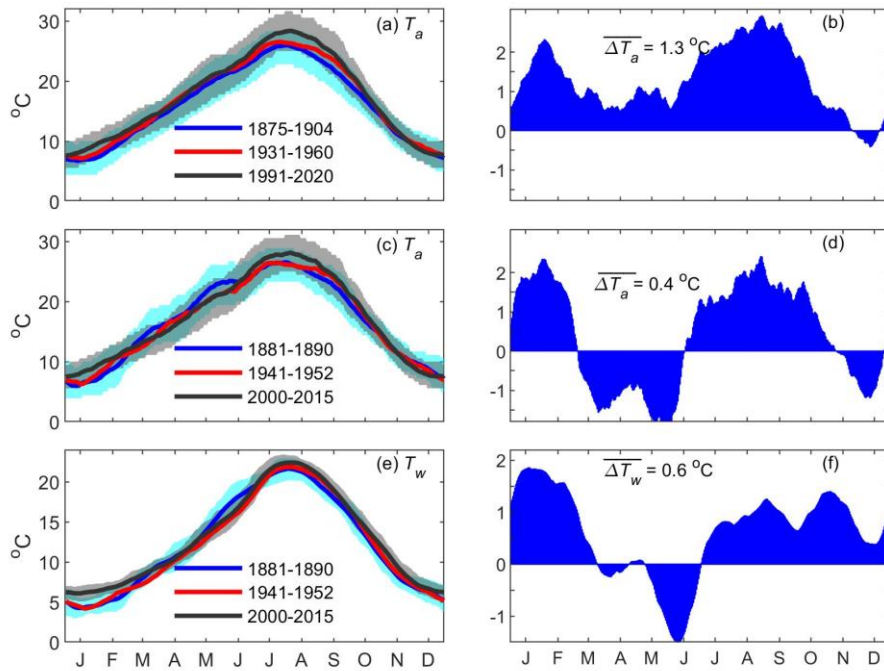


Figure 11: T_a and T_w climatology in Portland (a, c, e) and the difference between the modern (1991–2020) and historical period (1881–1890) in (b, d, f). Climatology is determined using a 30d moving average; shading denotes the 25th and 75th percentile of the measurements. A 30-year average is used in (a); the time periods for (c) and (e) are determined by the time period used to calibrate the T_w model. The tick marks on the x axis denote the middle of each month. The average T_w difference between the modern and earliest period is provided in (b, d, f).

Model results confirm that changes in T_a (driven by climate change, (increased T_a)) are the most significant factor in long-term increases in T_w , with net system changes an additional important contributor during the cool season (Figure 12). Seasonally, changes to T_a between the 1875–1904 and 1991–2020 periods dominate the modeled trends in T_w during late winter, summer and early fall (late January–early March, July–October) and in late winter (Figure 12). Averaged over a year, a total increase in T_w of 0.81 ± 0.25 °C is correlated to T_a changes. A maximum climate-induced change of $\sim 1.7 \pm 0.3$ °C occurs in September. Climate shifts produce a lesser shift of 0.5–0.6 °C increase in T_w in spring (late March to June), and little change occurs in December, consistent with air-temperature climatology (compare Figure 11 and 12). Interestingly, The uncertainty in the T_a air-temperature contribution is driven by the inherent 95% confidence uncertainty in the T_a air-temperature climatology, which is ± 0.22 °C, and is caused by interannual variability (see Equation 5); model coefficient uncertainty is a minor fac-

Formatted: Not Highlight

Formatted: Not Highlight

Formatted: Not Highlight

Formatted: Not Highlight

Formatted: Not Highlight

Formatted: Not Highlight

Formatted: Not Highlight

1044 ~~tor_w~~, rather than uncertainty in the model coefficients. Moreover, ~~m~~Modeled T_w changes are ro-
 1045 bust to ~~any~~ small systematic biases in T_a ; if the average change in T_a is reduced by 0.54 °C (con-
 1046 sistent with the Scott et al. 2023 estimate for Portland T_a change), the average T_w only decreases
 1047 by ~0.233 °C. Hence, we conclude that changes to the meteorological heat-balance (as repre-
 1048 sented by T_a) are the major cause of increasing T_w . ~~Consistent with our results, climate models~~
 1049 ~~also suggest that future summertime T_w in the Pacific Northwest will increase much more than~~
 1050 ~~T_w during other seasons, consistent with our results (Ficklen et al., 2014).~~

1051 Integrated Ssystem changes between the 1940s and today (defined in section 2.5) ~~–(as estimated~~
 1052 ~~by changing regression coefficients()~~ between the 1940s and today cause a T_w increase of ~0.5–
 1053 0.6 °C from November–May, ~~dropping to about~~ are statistically insignificant amount from late
 1054 June to early October (Figure 12). Averaged over a year, the total increase in T_w caused by sys-
 1055 tem change is 0.34 ± 0.12 °C ~~since the 1940s; no statistically significant influence between the~~
 1056 ~~1881 and 1941 era models was found, and is not shown.~~ The net change is caused by an altered
 1057 decorrelation structure between models from the 2000 and 1941 eras (Figure 3).

1058 ~~The observed seasonal shifts are consistent with an increased thermal inertia caused by the rever-~~
 1059 ~~voir system, as also discussed elsewhere (see e.g. Webb & Weber, 1993; Caissie 2006; Olden~~
 1060 ~~and Naiman, 2010). Effectively, heating or cooling from many months ago still influences T_w in~~
 1061 ~~the modern system, tending to elevate wintertime and depress summertime temperatures (see dis-~~
 1062 ~~cussion for other influences). In the statistical model, we find that monthly averaged T_a exerts a~~
 1063 ~~statistical influence on T_w for 4 months, compared to 3 months historically (not shown). The~~
 1064 ~~magnitudes of coefficients magnitudes at 2–4 months lags are also larger today, at -0.0025~~
 1065 ~~$^{\circ}T_w/^{\circ}T_a$ per day (modern) vs. $-0.0017^{\circ}T_w/^{\circ}T_a$ per day (1940s; annual model). The other signifi-~~
 1066 ~~cant change in the modern model is a lessened sensitivity to synoptic weather patterns, as ob-~~
 1067 ~~served by smaller coefficients at <7 days lag (Figure 3) and less variance (Figure 5). Both the de-~~
 1068 ~~creased sensitivity and the longer system memory in the modern system affect the modeled T_w ,~~
 1069 ~~leading to the changed pattern of T_w responses to atmospheric forcing.~~

1070 Changes in ~~the average river hydrograph or average river flow~~(Figure 2a) exert a minor influence
 1071 ~~on annually averaged T_w , but yet~~ are important for T_w during late summer. During July, a slight
 1072 increase in T_w is observed from changed river flow. In August and especially September, the de-
 1073 creases in T_w caused by increased flow releases, (-0.27 °C and -0.56 °C, respectively) are signifi-
 1074 cant. Thus, the release of water from reservoirs late in the summer ~~to some extent~~ counteracts, ~~to~~
 1075 ~~some extent~~, the effects of increased air temperatures (Figure 12). During other times of year, no
 1076 statistically significant modeled correlation between Q and T_w was found, likely because the av-
 1077 erage T_w gradient in the mainstem Willamette River is small (Figure 2b). While river flow may
 1078 be important in winter during times of large positive or negative temperature gradients, these
 1079 changes are likely transient and a process-based model would be required to ~~capture it~~ detect
 1080 ~~them~~. The net effect of summertime changes in ~~Q river flow~~ on the annual average is small: ~~A~~
 1081 total decrease in annually averaged T_w of ~0.05 °C is estimated.

Formatted: Not Highlight

Formatted: Not Highlight

Formatted: Font: Italic

Formatted: Font: Italic, Subscript

Formatted: Font: Italic

Formatted: Highlight

Formatted: Highlight

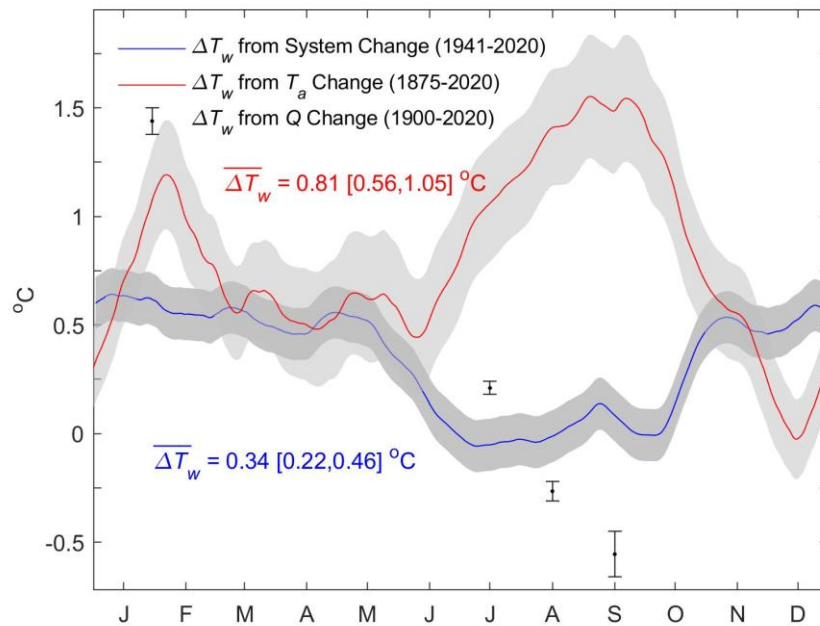


Figure 12: Estimated T_w changes caused by T_a (climate change), system changes (i.e., differences between the parameters of the modern and historic models), and discharge changes (July–September). A positive value indicates an increase over time. System changes are based on taking the difference in estimated T_w obtained over the 2000–2020 time period using the 1940s era model (model 1941A) and the modern era model (model 2000A). The influence of increased solar heating (climate change) is estimated by differencing the T_a and T_w values obtained with the 1941A model using the 1875–1904 and 1991–2020 T_a climatologies (Figure 11). Shading shows 95% uncertainty bounds and includes the combination of the both the 95% uncertainty in the mean climatology and the 95% uncertainty in the model coefficients. The July–September change in monthly averaged T_w produced by discharge is obtained by comparing the pre-reservoir (1901–1940) and the modern (1981–2020) hydrographs (Figure 2a) into the statistical model, with T_a forcing held constant. The uncertainty bounds for the influence of altered river flow error bars denote the difference in the 1941A and 2000A model estimates. See section 2.5 for details on calculations.

Overall, the sum of estimated temperature changes caused by climate, system, and water management changes since ~1900 ($\sim 1.1 \pm 0.3^\circ\text{C}$; Figure 12) is consistent with the overall long term trends in T_w of $1.1 \pm 0.2^\circ\text{C}$ per century (Figure 7a). T_a T_w . Thus, we conclude that ongoing climate

Formatted: Font: (Default) Times New Roman, 12 pt

Formatted: Font: (Default) Times New Roman, 12 pt

Formatted: Not Highlight

Formatted: Font: (Default) Times New Roman, 12 pt

Formatted: Not Highlight

Formatted: Font: (Default) Times New Roman, 12 pt

Formatted: Not Highlight

Formatted: Font: (Default) Times New Roman, 12 pt

Formatted: Not Highlight

Formatted: Font: (Default) Times New Roman, 12 pt

Formatted: Not Highlight

Formatted: Not Highlight

Formatted: Font: (Default) Times New Roman, 12 pt

Formatted: Highlight

change is the primary cause of increased temperatures, with system changes an important contributor. We note again that we cannot discern the influence of individual factors such as changed shading, river depth, storage, or snow pack, nor can we assess coupled, nonlinear changes. For example, changes to river flow may in part be caused by climate change, and alterations in T_w may in part be influenced by urbanization or deforestation. Nonetheless, the results provide insights into the causes of T_w change and why some parts of the year are subject to larger upward trends than others, over secular timescales.

Formatted: Highlight

4.0 Discussion

The observed annual trend in T_w of 1.1 ± 0.2 °C/century in the lower Willamette River is similar to the magnitude of change observed or estimated in the few studies available over similar time scales. For example, Moatar and Gailhard (2006) estimated a 0.8 °C increase in the Loire since 1881, Webb and Noblis (2007) estimated a change of 1.4–1.7 °C on Austrian rivers since ~1900, and Scott et al. (2020) (2023) estimated a trend of 1.3 °C/century for the nearby Columbia River to which the Willamette River is a tributary over the past 170 years (see also Scott et al., 2022). Similar to our results, studies also often highlight that the seasonal distribution of changes of T_w is unequal (e.g., Webb and Noblis, 2007). Consistent with our results, studies from the Pacific Northwest suggest that climate change and specifically the processes driving increased T_a (i.e., climate change) are also driving T_w trends over recent decades (Isaak et al., 2012). Future climate change will be expected to continue to increase T_a and drive T_w trends, with the largest increases in summer (Caldwell et al., 2013; Ficklin et al., 2014). Additionally, unimpeded discharge is expected to increase in winter and decrease in summer (e.g., Chang & Jung, 2010), which would also raise late summer T_w (Figure 12).

Formatted: Font: Italic

Formatted: Font: Italic, Subscript

Formatted: Not Highlight

4.1 Interpretation of T_w patterns

Ongoing air temperature changes are the primary cause of the modeled increase in water temperatures, with river system changes an important contributor (Figure 12). The sum of estimated temperature changes caused by climate, system, and water management changes from ~1900 to the present is $\sim 1.1 \pm 0.3$ °C (Figure 12) and is consistent with the overall long-term trends in T_w of 1.1 ± 0.2 °C per century (Figure 7a). Of modeled changes since ~1900, 0.81 ± 0.25 °C (74%) is caused by increased T_a , while 0.34 ± 0.12 °C (~31%) is caused by alterations in the T_w response to forcing (integrated river system change); river flow alteration produces a -5% change, closing the balance. Thus, we conclude that largest increases in Willamette water temperature are driven by climate change. This contrasts with the nearby Columbia River, in which flow regulation and other anthropogenic changes cause the majority of historical T_w shifts (Scott et al., 2023). One major difference is the percentage of water that is stored in reservoirs: approximately 40% of Columbia River flow is stored behind reservoirs, vs. about 10% for the Willamette.

Formatted: Font: Not Bold

Formatted: Font: Not Bold, Italic

Formatted: Font: Not Bold, Italic, Subscript

Formatted: Font: Not Bold

Formatted: Not Highlight

Formatted: Not Highlight

But, However, our results suggest that deepening of the river system has system changes have altered the response of T_w to climate change meteorological forcing, and in particular to and weather climate extremes, producing less water temperature variance (Figure 5 & 6) and an altered decorrelation structure in model coefficients (Figure 3), as explored below. At short time lags of 0–5 days, historical model coefficients are as much as 2–3x larger than modern coeffi-

cients, indicating more sensitivity to air temperature fluctuations (Figure 3) In the modern system, increased depth d reduces the effect of atmospheric heating H , leading to smaller $\frac{\partial T_w}{\partial t}$ and smaller coefficients (see Equation 1; Caissie, 2006). Depth increases are driven by the reservoir system, which is known to decrease T_w variability in the Willamette on 1–8 day time scales (Steel and Lange, 2007). The change from braided, shallow channels to a single, deeper channel is also likely influential (see Section 2.1).

Formatted: Not Highlight

Formatted: Not Highlight

Formatted: Not Highlight

The changing correlation structure (Figure 3) and the influence of increasing depth has implications for how extremes in a changing climate are observed. Specifically, a historical heat wave in T_a was likely to produce a larger change in T_w than it would today. The record-breaking, climate-change influenced heat wave in July 2021 (e.g., White et al., 2023), with a high T_a of 46.7 °C, did not cause a record T_w . Despite T_a values exceeding the previous all-time high by nearly 5 °C, morning water temperature peaked just over 24 °C, approximately 2 °C below the largest recorded (as discussed in section 2.2, we use morning measurements in our model). A similar process mitigates the effect of cold air events, and helps keep modern water temperatures above freezing (Figure 7). Effectively, T_w in the modern system has become more resilient to extreme heat waves or cold weather anomalies.

Formatted: Not Highlight

Another reason for historical T_w variability in winter was the occasional occurrence of deep freezes that no longer occur. During the winters of 1861–62 and 1867–1868, for example, T_a remained below 0 °C for 32 and 31 days, respectively, and newspapers recorded ice-skating on the lower Willamette River. Navigation in Portland Harbor was halted or hindered by ice from New Year’s Day until mid-March, 1862. No 20th century winter matched the duration or severity of these events, though 18–19 freezing days (daily maximum below 0 °C) were recorded in 1915–1916, 1929–1930, and 1949–1950. In 1979, air temperatures remained below 0 °C for a total of 14 days; since 1980, no winter has produced more than 9 sub-freezing days. On average, the statistical variability of air temperature from its climatological mean is similar today as historically (Figure 5); however, the frequency of extreme cold-waves (e.g., 1 in 10 year events) has decreased over the past century (Vose et al., 2017). The average coldest day of the year is now ~2.7 °C warmer in the Pacific Northwest than during the first half of the 20th century, far outpacing the annual average increase of 1.1 °C since 1900 (Vose et al., 2017, Mote et al., 2019). Both increasing average winter air temperatures and decreasing cold extremes help explain upward trends in bi-monthly averaged temperatures (Figure 6) and seasonal minima (Figure 7b). For example, the year-to-year variation in average Jan-Feb T_w was 0–6 °C during the 19th century, and is 5–8 °C today (Figure 6). During winter, the shallower historical streams may have contributed to the ice formation observed during some 19th century winters. Thus, changing meteorological forcing combines together with altered system response to increase wintertime temperatures but reduce variance (Figure 12).

Formatted: Not Highlight

Formatted: Not Highlight

Formatted: Not Highlight

Formatted: Not Highlight

Formatted: Not Highlight

Formatted: Superscript, Not Highlight

Formatted: Not Highlight

Formatted: Not Highlight

Formatted: Font: Italic, Not Highlight

Formatted: Not Highlight

Formatted: Superscript, Not Highlight

Formatted: Not Highlight

Formatted: Not Highlight

Formatted: Not Highlight

The integrated effect of weather during previous months is more important today than historically. At lags of >2 weeks, coefficient magnitudes are ~50% larger in the modern models (see section 3.1). Hence, the thermal memory of the system to T_a anomalies lasting a month or longer is larger. Nonetheless, the influence of each individual day at lags >2 weeks is small (see Figure 30, and only the integrated, monthly averaged effect is important. Hence, increased thermal memory smooths out variability and keeps the system closer to climatological conditions. Thermal memory (thermal inertia) also elevates wintertime and depresses summertime temperatures

Formatted: Not Highlight

(e.g., Figure 12). Similar patterns have been observed elsewhere and attributed to water regulation and storage (see e.g. Webb & Weber, 1993; Caissie 2006; Olden and Naiman, 2010), but can be also influenced by the time-lag effects of snowmelt.

Formatted: Not Highlight

The observed seasonal shifts are consistent with an increased thermal inertia caused by the reservoir system, as also discussed elsewhere (see e.g. Webb & Weber, 1993; Caissie 2006; Olden and Naiman, 2010). Effectively, heating or cooling from many months ago still influences T_w in the modern system, tending to elevate wintertime and depress summertime temperatures (see discussion for other influences). Both measurements (e.g., Figure 5) and the statistical model coefficients for T_a (Figure 3) suggest that the sensitivity of T_w to short-term meteorological forcing has decreased over time. A major cause is the reservoir system, which is known to decrease T_w variability in the Willamette on 1–8 day time scales (Steel and Lange, 2007). At short time lags of 0–5 days, historical model coefficients are as much as 2–3x larger than modern coefficients (Figure 3). Therefore, a historical heat wave in T_a was likely to produce a larger change in T_w than today. Simultaneously, the integrated effect of weather during previous months is more important. At lags of > 2 weeks, coefficient magnitudes are ~50% larger in the modern models than historically. Hence, the thermal memory of the system to T_a anomalies lasting a month or longer is larger. Thermal memory stems from storage effects, whether from the heat stored in reservoirs (Webb & Weber, 1993; Caissie, 2006; Olden & Naiman, 2010) or the cooling effects of snow melt and groundwater in summer, which together are the primary source of water during this period (Brooks et al., 2012). The net thermal memory has increased, providing a buffering effect that helps explain why both seasonal and interannual variations in T_w are less pronounced today.

We attribute the decreased sensitivity of T_w to short-term, synoptic weather patterns (< 1 week) to a system-wide increase in depth, caused by the reservoir system (Rounds, 2007, 2010) and by channelization and depth increases in the river (Sedell & Froggatt, 1984; Gregory et al., 2002a). A larger depth d decreases the magnitude of the heating term ($\frac{H}{\rho c_p d}$) in Equation (1), leading to smaller temperature change in the leading order balance $\frac{\partial T_w}{\partial t} = \frac{H}{\rho c_p d}$. This explains the decrease in model coefficients for small time lags (< 1 week). Reservoirs in the upper watershed increase the mean depth of the entire system, reducing the overall rate of temperature change but and increasing heat storage capacity (Caissie, 2006). Similarly, the transition from a multi-braided stream to a dredged river with one primary channel also contributes to increased depth, to an unknown extent. Gravel mining and dredging for the harbor may also have increased depths in the lower Willamette (see e.g., Jay et al., 2011). These Portland region depth increases may be offset by a decrease in backwater effects from the Columbia River, particularly in spring (Helaire et al., 2019).

The changing correlation structure (Figure 3) and the influence of increasing depth has implications for how climate change effects are observed. At short time scales (< 1 week), the decreased modern sensitivity to T_a air temperature perturbations (Figure 3) implies that depth increases outweigh altered H in the heating term. If the correlation structure had remained unchanged, a 1°C step increase in T_a would result in a larger short-term perturbation than is currently observed. Hence, T_w in the modern system has become more resilient to extreme heat waves. The record

Formatted: Highlight

1228 breaking heat wave in July 2021, with a high T_a of 46.7 °C, did not cause a record T_w . Despite
 1229 T_a air temperature values exceeding the previous all-time high by ~5 °C, the daily minimum max-
 1230 imum water temperature T_{ws} peaked just over 24 °C, in part because the heat wave was shorter
 1231 than other events. We conclude that water temperature T_{ws} are is now more influenced by cli-
 1232 mate change induced changes to T_a air temperature climatology and long-time scale pattern term
 1233 trends, rather than short-term extreme events.

1234 Numerical, process-based models run over a smaller shorter time-scale duration provide addi-
 1235 tional clues to the factors driving long-term changes. For example, loss of shading (86%) and
 1236 secondarily because of point-source discharges (e.g., from water treatment plants ~ 14%) in-
 1237 creased non-reservoir anthropogenic factors were modeled to increase Willamette River water
 1238 temperatures in Portland by 0.3 ± 0.05 °C between June and October of 2001 (OR
 1239 DEQ, 2006), primarily due to loss of shading (86%) and secondarily because of point source
 1240 discharges (e.g., from water treatment plants). The same CE2-Qual model determined a reduc-
 1241 tion of approximately 0.1 °C for each additional 100 m³/s of river flow released into the lower
 1242 Willamette. This is consistent though not identical with our modern statistical model, which pro-
 1243 duces suggests an average decrease influence of ~-0.07 °C for each extra 100 m³/s of river flow.
 1244 ow, spread out over several months via the decorrelation structure (Figure 3d).

1245
 1246 River discharge is found to only be influential on T_w during summer (see also Isaak et al., 2012),
 1247 and is River flow effects on T_w are likely driven by the substantial increase in water temperature
 1248 along the river observed during July-September (positive summertime $\frac{dT_w}{dx}$). (Figure
 1249 2b). Another factor during July-September, but are also influenced by is the increased velocity
 1250 u and river depth d caused by each incremental increase regulated releases of water in discharge.
 1251 Larger river flow increases the rate at which cooler water is moved downstream (increased $u \frac{\partial T_w}{\partial x}$)
 1252 and also diminishes the contribution from surface heating on temperature (smaller $\frac{H}{\rho c_p d}$; see
 1253 Equation 1). The large increase in September discharge compared to historical conditions (Figure
 1254 2) reduces temperatures by 0.56 °C, a larger amount more than in August (Figure 12). In Octo-
 1255 ber, average $\frac{\partial T_w}{\partial x} - \frac{dT_w}{dx}$ becomes small (Figure 2), and managed releases are unlikely to reduce wa-
 1256 ter temperature. After September, our approach is unable to find a statistically significant influ-
 1257 ence of river discharge.

1258 Interestingly, the overall river system was less sensitive to river flow fluctuations in the 1940s
 1259 (Figure 3d), and no statistically significant effect of river flow was observed in the 1880s. The
 1260 lack of correlation in the 1880s may simply reflect imperfect-incomplete flow estimates (see ex-
 1261 planation in Jay & Naik, 2011). A dynamical explanation remains speculative without a process-
 1262 based retrospective model using historical bathymetry. However, some factors may have re-
 1263 duced average summertime river flow influences ($u \frac{dT_w}{dx}$) historically (Equation 1). Compared to
 1264 today, the Nonetheless, it is possible that the bottomland forests and braided river networks of
 1265 the historical Willamette River greatly probably reduced $\frac{dT_w}{dx}$, velocity u , and the longer
 1266 river length slightly reduces $\frac{dT_w}{dx}$ (see section 2.1). Cold groundwater discharges, which are

Formatted: Not Highlight

Formatted: Not Highlight

known to occur in off-main channel alcoves and were more connected to the river historically (e.g., Faulkner et al., 2020), may have reduced surface heating effects. Riparian shading similarly reduced heating (OR DEQ, 2006). Nonetheless, understanding the relative importance of these factors requires additional research, and the advective heating term during summer (Equation 1), producing the observed lack of correlation. Mechanisms that might be influential include stream width changes (e.g., White et al., 2017) and cold groundwater discharges, which is known to occur in off-main channel alcoves (e.g., Faulkner et al., 2020). During winter, the shallower historical streams may have contributed to the freezing water temperatures observed during some years in the 19th-century winters. A process-based retrospective model using historical bathymetry would be required to further investigate these conjectures, and determine the relative roles of geomorphic change, ecological change, and the reservoir system on T_w .

4.2 Implications

Since spring T_w values are less changed than summer values (Figure 11), less extra heat is input at the beginning of the warm season, and warm T_w is not biased early in the modern record. In the late summer, reservoir releases are tamping T_w values downwards (Figure 12).

The increase in the number of days that temperatures exceed established thresholds has been observed in other river systems (e.g., Markovic et al., 2013) and is projected to continue in the Pacific Northwest (Mantua, 2010). Our observations show that the rate of change is threshold-dependent, and slows as the accumulated number of days above a threshold becomes large. Therefore, the number of days over 20 °C (which is already large) is increasing less quickly than the number of 22 °C days, which occur primarily during mid-summer (Figure 9). Effectively, exceedances of lower thresholds like 18 °C and 20 °C are limited by spring and fall, when climatological values of T_{air} and water temperature T_{ws} change quickly (note that spring-time water temperature T_{ws} are also held lower by thermal memory). Conversely, in winter, the largest rates of change are observed for larger levels of exceedance; hence, the number of cold-water days below 4 °C is decreasing faster than those below 2 °C. Both the decreased spread in water temperatures (Figure 5) and increased mean temperatures (Figure 6 & 7) drive the large change in the number of days below 4 °C. Increases in winter T_w minima and averages are not a focus of regulation, but are ecologically important (e.g., Webb & Weber, 1993; Caissie, 2006). For example, cold water events and wintertime conditions influence the survivability and recruitment of fish by altering their biotic interactions, habitat use, physical condition, feeding rates, and community structure (see reviews by Hurst 2007; Brown et al., 2011; Weber et al., 2013). It is also possible that historical wintertime conditions, such as the deep freezes discussed above, provided some protection against non-native plants and fauna that thrive in warmer waters.

Average temperatures in Jan–Feb, the period with the coldest temperatures, have increased from ~0–6 degrees to 5–8 degrees (Figure 6a). Hence, both the decreased spread in temperatures (Figure 5) and the increased mean drive the large change in the number of days below 4 °C.

Compared to historical norms, water temperature T_{ws} today exhibits less lower variability, both day-to-day and between annual the maximum and minimum values. (both climatology and daily extrema). A result is that temporal refugia—which we define as time periods in which water

Formatted: Not Highlight

1308 temperature T_w s temporarily dips below biologically important thresholds such as 18 °C or 20
 1309 °C—are becoming less frequent (see Figures 9 & 10). Hence, while the management practice of
 1310 selectively releasing river water is successfully reducing average temperatures in late summer
 1311 (Figure 12), it may not be addressing the decrease in variance (e.g., Figure 5) caused by system
 1312 changes. Because some migrating fish such as steelhead delay migration during warm periods
 1313 by weeks or months, likely causing increased mortality (e.g., Siegel et al., 2021), ~~the a reduced~~
 1314 ~~reduction in~~ temporal refugia ~~are-is potentially~~ important ~~to consider~~ (see also Steel et al., 2012).
 1315 At Portland, T_w exceeds ~~biologically important thresholds during some part of every year—and~~
 1316 ~~has done so throughout the period of record did so even in the 19th century—biologically im-~~
 1317 ~~portant thresholds during some part of every year.~~ However, the more consistently warm river
 1318 temperatures during summer and ~~the shoulder seasons~~ autumn—as observed by the increase in
 1319 ~~the~~ time over 18 °C and 20 °C—likely creates a thermal barrier, ~~that has~~ with implications for
 1320 salmon migration (see e.g., Notch et al., 2020).

1321 4.3 Study Limitations

1322 Statistical models are fast, can be applied to large time scales, and provide insights into the major
 1323 factors influencing water temperature (e.g., Benyahya et al., 2007). Nonetheless, factors such as
 1324 wind, heating, evaporation, time or spatial variation in parameters, and alterations in depth are
 1325 only approximately represented by T_a , T_w and Q . At different times, various terms (e.g., depth,
 1326 heat flux, and velocity) may contribute in varying degrees to the overall heat balance (Equation
 1327 1), leading to a different statistical relationship between forcing variables and T_w . We address
 1328 this issue by developing summer, winter, and annual sub-models, and by developing models for
 1329 different eras (Figure 3). Nonetheless, river system and climate changes occurred continuously
 1330 over the period of record, making application of the models to different time periods only ap-
 1331 proximate. For example, managed releases of water for temperature control became more preva-
 1332 lent in the late 1990s (National Research Council, 2004), and may decrease the hindcast skill of
 1333 our 2000 era model for earlier periods. The quality and spatial variability of data used in the
 1334 model may also affect conclusions. If we use a 0.9 °C increase in air temperature since 1900
 1335 (following Scott et al., 2023), rather than 1.3 °C, the estimated influence of T_a on T_w is reduced
 1336 by 0.23 °C. Nonetheless, our results are generally consistent between models (section 3.1), and
 1337 any small biases or uncertainties in the data only shift the details, but not the main conclusions,
 1338 of the study.

1339 Our approach cannot discern the influence of individual factors such as changed shading, river
 1340 depth, storage, or snow pack, nor can we assess coupled, nonlinear changes. For example,
 1341 changes to river flow (Figure 2) may in part be caused by both climate change, land use, and wa-
 1342 ter management (e.g., Swain et al., 2021, Liang et al., 2020), and alterations in T_a may in part be
 1343 influenced by urbanization or deforestation. A numerical modeling approach is needed to isolate
 1344 individual anthropogenic stressors and to determine how landscape and climate changes can in-
 1345 fluence T_w in incremental, nonlinear, and interdependent ways (e.g., Berger et al., 2004). None-
 1346 theless, our results provide insights into the causes of T_w change and why some parts of the year
 1347 are subject to larger upward trends than others, over secular timescales. 🟡

Formatted: Superscript

Formatted: Not Highlight

Formatted: Not Highlight

Formatted: Not Highlight

Formatted: Not Highlight

Formatted: Font: Italic

Formatted: Font: Italic, Subscript

Formatted: Font: Italic

Formatted: Font: Italic

Formatted: Font: Italic, Subscript

Formatted: Font: Italic

Formatted: Space After: 18 pt

Formatted: Not Highlight

Formatted: Highlight

Formatted: Font:

5.0 Conclusion

5.0 Conclusion

In this contribution, we found, digitized, produced, and quality controlled a 90-year long T_w record (1881–~~1890, 1941~~–2021) for the lower Willamette River in Portland, Oregon. The in-situ measurements enabled the development of statistical T_w models based on the 1880s, 1940s, and modern time periods. Subsequently, estimates of daily minimum T_w for the years 1850–2021 ~~are were~~ produced using daily measurements of maximum T_a and river discharge. A good comparison between measurements and models is observed (~~Table 2~~), with RMSE similar to numerical models, including cool-season T_w water temperature measurements (November–April) in the Columbia River Estuary from 1854–1876.

Water temperature ~~Water temperatures~~ are increasing throughout the year (average trend of 1.1 ± 0.2 °C/century), with the largest ~~trends increase~~ observed in winter. As a result, the number of cold-~~water~~ days per year is ~~precipitously~~ declining, while the number of days above 20 °C has increased by an average of ~ 20 d yr⁻¹ (~~Figure 10~~). The primary cause of changed T_w since ~ 1900 is climate change (0.84 °C), followed by system changes such as the building of reservoirs, loss of shading, and other landscape alterations (0.34 °C; ~~Figure 12~~). Changes ~~and reductions in flow~~ river discharge have a generally smaller influence, except during managed releases in late summer.

Ongoing climate changes (as observed through air temperature increases) are the primary cause of increased water temperatures, with river system changes an important contributor, particularly during winter. Because of a larger heat capacity and greater system depth, the day-to-day variability in T_w has decreased and the sensitivity to heat waves or cold snaps is diminished. ~~(e.g., Figure 5) These changes are observed in model coefficients and in a reduced variance from the climatological mean. Thus, Even though average temperatures in summer are now highelarger than historically, but peak annual maximum temperatures have changed lessare (more) similar.~~ Hence, warm summers marked by low river flow produced similar peak temperatures in 1889, 1941, and 2015 (~~Figure 9~~), and but a truly n-extreme heat wave in 2021 did not produce record T_w ~~water temperatures values, possibly because of its short duration. Notably, the Portland heat-wave of record before 2021 (5d above 37.8 °C in 1941) produced higher maximum T_w than either 2015 or 2021, but not a prolonged period of extreme T_w . The relative suppression of peak T_w has been bought at the expense of daily and interannual variability; during most times of the year, but particularly in winter, there is less day to day variation than in the 19th century. River system alterations and climate change have greatly increased winter temperatures and reduced year-to-year variability, and Climatically meteorologically induced disturbance events such as freezing rarely occur anymore. Similarly, temporal refugia—time periods in which T_w dips below biologically important warm water thresholds for over heating have also decreased (Figures 9 & 10). Therefore, Temporal refugia during the time period for a most conducive to coldwater species pe-ies require are becoming increasingly scarce, especially during summer.~~ These system changes may pose a grave threat to endemic species, should climate-induced changes in T_w continue.

Formatted: Not Highlight

Formatted: Not Highlight

Formatted: Not Highlight

Formatted: Not Highlight

1388

1389 Data Availability

1390 The T_w water temperature data used in the research is available upon request, and will be up-
1391 loaded to a data repository upon acceptance of the manuscript have been archived in the Portland
1392 State University depository (<https://doi.org/10.15760/cee-data.06>). Meteorological data are
1393 available from the National Centers for Environmental Information
1394 (<https://www.ncei.noaa.gov/>). Pre-1890 Vancouver and Portland records were also obtained
1395 from the Midwestern Regional Climate Center (https://mrcc.illinois.edu/data_serv/cdmp/cdmp.jsp). River flow records are obtained from the US Geological
1396 Survey and the sources described in section 2.2.

Formatted: Font: (Default) Times New Roman, 12 pt

1398 Author Contribution

1399 SAT found and processed archival data, conceptualized research question, developed the statisti-
1400 cal model, analyzed results, produced figures, and was primary lead on drafting the paper. DAJ
1401 developed an earlier version of the model and assisted with research questions, interpretation and
1402 paper development. HLD assisted with conceptualizing research questions, interpretation, litera-
1403 ture review, and paper drafts development, and helped secure funding.

1404 Competing Interests

1405 The authors declare that they have no conflict of interest

1406 Acknowledgements

1407 Funding was provided by Bonneville Power Administration, under Project No. 2002-077-00 with
1408 the Pacific Northwest National Laboratory, and by the US National Science Foundation, CA-
1409 REER Award 1455350 and NSF project 2013280. Margaret McKeon is thanked for her help de-
1410 fining the watershed boundaries in Figure 1, and students at Portland State University are
1411 thanked for helping to digitize and quality assure the 1854-1876, 1881-1890, and 1941-1961 ~~wa-~~
1412 ~~ter temperature~~ T_w records used in this study.

1413

References

- Al-bahadily, A.: Long Term Changes to the Lower Columbia River Estuary (LCRE) Hydrodynamics and Salinity Patterns. PhD thesis. Portland State University, doi: 10.15760/etd.7357, 2020.
- Al-Murib, M. D., Wells, S. A., and Talke, S. A.: Integrating Landsat TM/ETM+ and numerical modeling to estimate ~~water temperature~~ ~~water temperature~~ in the Tigris River under future climate and management scenarios. *Water*, 11(5), 892, doi.org/10.3390/w11050892, 2019.
- Angilletta M.J., Steel E.A., Bartz K.K., Kingsolver J.G.,Scheurell M.D., Beckman B.R., and Crozier L.G.: Big dams and salmon evolution: changes in thermal regimes and their potential evolutionary consequences. *Evolutionary Applications*,1, 286–299, doi: 10.1111/j.1752-4571.2008.00032.x, 2008.
- Annear, R., McKillip, M., Khan, S. J., Berger, C., and Wells, S.: Willamette Basin Temperature TMDL Model: Boundary Conditions and Model Setup, Technical Report EWR-03-03, Department of Civil and Environmental Engineering, Portland State University, Portland, Oregon, 2003.
- Baker, J., Van Sickle, D., White, D.: Water Sources and Allocation. In: Willamette River Basin Planning Atlas (D. Hulse, S. Gregory and J. Baker, Eds.), pp. 40–43. Oregon State University Press, Corvallis, 2002.
- Benyahya L., Caissie,D.,St-Hilaire, A., Ouarda, T.B.M.J., and B. Bobée.: A Review of statistical ~~water temperature~~ ~~water temperature~~ models. *Canadian Water Resources Journal*, 32(3), 179-192, doi.org/10.4296/cwrj3203179, 2007.
- Benner, P., and Sedell, J.: Upper Willamette River Landscape: A Historic Perspective. In *River Quality: Dynamics and Restoration*. Ed. Antonius Laenen and David A. Dunnette. Boca Raton: CRC/Lewis, 23-46, 1997.
- Berger, C., McKillip, M.L., Annear, R.L., Khan, S.J., and Wells, S.A.: Willamette Basin Temperature TDML Model: Model Calibration. Portland State University, Department of Civil and Environmental Engineering. Technical Report EWR-02-04, 2004.
- Branscomb,A., Goicochea J., and Richmond, M.: Stream Network. In: Willamette River Basin Planning Atlas (D. Hulse, S. Gregory and J. Baker, Eds.), pp.16-17. Oregon State University Press, Corvallis, 2002.
- Brooks, J. R., Wigington, P. J., Phillips, D. L., Comeleo, R., and Coulombe, R.: Willamette River Basin surface water isoscape (δ 18O and δ 2H): temporal changes of source water within the river, *Ecosphere*, 3, 39, doi:10.1890/ES11-00338.1, 2012.
- Brown, R. S., Hubert, W. A., and Daly, S. F.: A primer on winter, ice, and fish: what fisheries biologists should know about winter ice processes and stream-dwelling fish. *Fisheries*, 36(1), 8-26, doi.org/10.1577/03632415.2011.10389052, 2011.
- Bumbaco, K. A., Dello, K.D., and Bond, N.A.: History of Pacific Northwest Heat Waves: Synoptic Pattern and Trends. *Journal of Applied Meteorology and Climatology*, DOI:10.1175/JAMC-D-12-094.1, 2013.
- Bottom, D., Baptista, A., Burke, J., Campbell, L., Casillas, E., Hinton, S., Jay, D.A., Lott, M. A., McCabe, G., McNatt, R., Ramirez, M., Roegner, G. C., Simenstad, C. A., Spilseth, S., Stamatiou, L., Teel, D. and Zamon, J. E.: Estuarine habitat and juvenile salmon: Current and historical linkages in the Lower Columbia River and estuary. Final report, 2002-

2008. Report of the National Marine Fisheries Service to the U.S. Army Corps of Engineers. Portland, Oregon. Available at <https://www.nwfsc.noaa.gov/publications/index.cfm>, 2011.

Boyd, Robert, ed. *Indians, Fire, and the Land in the Pacific Northwest*: Corvallis: Oregon State University Press, 1999.

Caissie, D., El-Jabi, N. and St-Hilaire, A.: Stochastic Modelling of ~~water temperature~~*Water Temperatures* in a Small Stream Using Air to Water Relations. *Canadian Journal of Civil Engineering*, 25, 250–260, doi.org/10.1139/197-091, 1998.

Caissie, D.: The thermal regime of rivers: a review. *Freshwater Biology*, 51, 1389–1406, doi.org/10.1111/j.1365-2427.2006.01597.x, 2006.

Caldwell, R.J., Gangopadhyay, S., Bountry, J., Lai, Y. and Elsner, M.M.: Statistical modeling of daily and subdaily stream temperatures: Application to the Methow River Basin, Washington. *Water Resources Research*, 49, 4346 – 4361, doi.org/10.1002/wrcr.20353, 2013.

Chang, H., and Jung, I. W.: Spatial and temporal changes in runoff caused by climate change in a complex large river basin in Oregon. *Journal of Hydrology*, 388(3), 186–207, doi.org/10.1016/j.jhydrol.2010.04.040, 2010.

Christy, J.A. and Alverson, E.R.: ~~2011~~. Historical vegetation of the Willamette Valley, Oregon, circa 1850. *Northwest Science*, 85(2), pp. 93–107, <https://doi.org/10.3955/046.085.0202>, 2011.

Clemens B, Schreck C, van de Wetering S, and Sower S.: The potential roles of river environments in selecting for stream- and ocean-maturing Pacific lamprey, *Entosphenus tridentatus* (Gairdner, 1836). Pages 299– 322 in Orlov A, Beamish R, editors. *Jawless fishes of the world. Volume 1*. Newcastle upon Tyne, UK: Cambridge Scholars Publishing.

Clemens, B. J.: Warm water temperatures ($\geq 20^{\circ}\text{C}$) as a threat to adult Pacific lamprey: Implications of climate change. *Journal of Fish and Wildlife Management* 13:1–8, DOI:10.3996/JFWM-21-087, 2022

Cloern, J. E., N. Knowles, L. R. Brown, D. Cayan, M. D. Dettinger, T. L. Morgan, D. H. Schoellhamer, M. T. Stacey, M. van der Wegen, R. W. Wagner, and A. D. Jassby.: Projected evolution of California’s San Francisco Bay-Delta-River System in a century of climate change. *PLoS ONE*, 6(9), e24465, doi:10.1371/journal.pone.0024465, 2011.

Crozier, L. G., Siegel, J. E., Wiesebron, L. E., Trujillo, E. M., Burke, B. J., Sandford, B. P., and Widener, D. L.: Snake River sockeye and Chinook salmon in a changing climate: implications for upstream migration survival during recent extreme and future climates. *PloS one*, 15(9), e0238886, doi.org/10.1371/journal.pone.0238886, 2020.

Donato, M.M.: A Statistical Model for Estimating Stream Temperatures in the Salmon and Clearwater River Basins, Central Idaho. US Geological Survey Water Resources Investigations Report 2002-4195, 2002.

Dugdale, S. J., Hannah, D. M., and Malcolm, I. A.: River temperature modelling: a review of process-based approaches and future directions. *Earth Sci. Rev.* 175, 97–113. doi: 10.1016/j.earscirev.2017.10.009, 2017.

Erickson, T. R. and Stefan, H. G.: Linear air/~~water temperature~~*water temperature* correlation for streams during open water periods. *Journal of Hydrologic Engineering*, 5(3), 317–321, doi.org/10.1061/(ASCE)1084-0699(2000)5:3(317), 2000.

Formatted: Font: (Default) Times New Roman, 12 pt

Formatted: Indent: Left: 0", Hanging: 0.5", Space After: 6 pt, Line spacing: single

Formatted: Font: (Default) Times New Roman, 12 pt

Formatted: Font: (Default) Times New Roman, 12 pt

Formatted: Font: Not Italic

Formatted: Font: Not Italic

1503 Faulkner B.R., Brooks J.R., Keenan D.M., and Forshay K.J.: Temperature Decrease along
1504 Hyporheic Pathlines in a Large River Riparian Zone. *Ecohydrology*. 4:13(1), 1-10. doi:
1505 10.1002/eco.2160. PMID: 32983317; PMCID: PMC7513865, 2020.

1506 Ficklin, D. L., Barnhart, B. L., Knouft, J. H., Stewart, I. T., Maurer, E. P., Letsinger, S. L. and
1507 Whittaker, G. W.: Climate change and stream temperature projections in the Columbia
1508 River basin: habitat implications of spatial variation in hydrologic drivers. *Hydrol. Earth*
1509 *Syst. Sci.*, 18, 4897–4912, <https://doi.org/10.5194/hess-18-4897-2014>, 2014.

1510 Fischer, H.B., List, E.J., Koh, R.C.Y., Imberger, J., and Brooks, N.H.: Mixing in inland and
1511 coastal waters. New York: Academic, 1979.

1512 Gregory, S., Ashkenas, L., Oetter, D., Minear, P., and Wildman, K.: Historical Willamette River
1513 Channel Change. In: Willamette River Basin Planning Atlas (D. Hulse, S. Gregory and J.
1514 Baker, Eds.), pp. 18-25. Oregon State University Press, Corvallis, 2002a.

1515 Gregory, S., Ashkenas, L., Oetter, D., Wildman, R., Minear, P., Jett, S., and Wildman, K.: Revet-
1516 ments, In: Willamette River Basin Planning Atlas (D. Hulse, S. Gregory and J. Baker,
1517 Eds.), pp. 32–33. Oregon State University Press, Corvallis, 2002b.

1518 Gregory, S., Ashkenas L., Jett, S., and Wildman, R.: Flood inundations/FEMA floodplains. In:
1519 Willamette River Basin Planning Atlas (D. Hulse, S. Gregory and J. Baker, Eds.), pp. 28–
1520 29. Oregon State University Press, Corvallis, 2002c.

1521 Gregory, S., Ashkenas L., Oetter, D., Minear, P., Wildman, K., Christy, J., Kolar, S., and Alver-
1522 son, E.: Presettlement Vegetation ca. 1851. In: Willamette River Basin Planning Atlas
1523 (D. Hulse, S. Gregory and J. Baker, Eds.), pp. 38–39. Oregon State University Press, Cor-
1524 vallis, 2002d.

1525 Gregory, S., Ashkenas, L., Haggerty, P., Oetter, D., Wildman, K., Hulse, D., Branscomb, A. and
1526 Van Sickle, J.: Riparian vegetation, In: Willamette River Basin Planning Atlas (D. Hulse,
1527 S. Gregory and J. Baker, Eds.), pp. 40–43. Oregon State University Press, Corvallis,
1528 2002e.

1529 Gregory, S.V., Frederick J. Swanson, W. Arthur McKee, Kenneth W. Cummins, An Ecosystem
1530 Perspective of Riparian Zones: Focus on links between land and water, *BioScience*, ~~Vol-~~
1531 ~~ume 41, Issue 8~~41(8), Pages 540–551, <https://doi.org/10.2307/1311607>, 1991.

1532 Gregory, S., Wildman, R., Hulse, D., Ashkenas, L. and Boyer, K.: Historical changes in hydrol-
1533 ogy, geomorphology, and floodplain vegetation of the Willamette River, Oregon. *River*
1534 *Research and Applications*, 35(8), pp. 1279-1290, <https://doi.org/10.1002/rra.3495>, 2019.

1535 Hamlet, A. F. and Lettenmaier, D. P.: Effects of climate change on hydrology and water re-
1536 sources in the Columbia River Basin. *JAWRA Journal of the American Water Resources*
1537 *Association*, 35(6), 1597-1623, <https://doi.org/10.1111/j.1752-1688.1999.tb04240.x>,
1538 1999.

1539 Helaire, L.T., Talke, S.A., Jay, D. A. and Mahedy, D.: Historical changes in Lower Columbia
1540 River and Estuary Floods and Tides. *Journal of Geophysical Research*, 124(11).
1541 <https://doi.org/10.1029/2019JC015055>, 2019.

1542 Hudson, A.S., Talke, S.A., and Jay, D.A.: Using satellite observations to characterize the re-
1543 sponse of estuary turbidity maxima to external forcing. *Estuaries and Coasts*, 39(5).
1544 DOI 10.1007/s12237-016-0164-3, 2017.

1545 Hurst, T. P.: Causes and consequences of winter mortality in fishes. *Journal of Fish Biol-*
1546 *ogy*, 71(2), 315-345, doi.org/10.1111/j.1095-8649.2007.01596.x, 2007.

Formatted: Font: (Default) Times New Roman, 12 pt

Formatted: Font: (Default) Times New Roman, 12 pt

Formatted: Font: (Default) Times New Roman, 12 pt

Formatted: Font: (Default) Times New Roman, 12 pt

Formatted: Font: (Default) Times New Roman, 12 pt, Not Italic

Formatted: Font: (Default) Times New Roman, 12 pt

Formatted: Font: Not Italic

Jay, D.A., and Naik, P.K.: Distinguishing Human and Anthropogenic Influences on Hydrological Disturbance Processes in the Columbia River, USA. *Hydrological Sciences Journal*, 56(7), 1186-1209, <https://doi.org/10.1080/02626667.2011.604324>, 2011.

Jay, D. A., Leffler, K., and Degens, S.: Long-term evolution of Columbia River tides. *Journal of Waterway, Port, Coastal, and Ocean engineering*, 137(4), 182-191, [doi.org/10.1061/\(ASCE\)WW.1943-5460.0000082](https://doi.org/10.1061/(ASCE)WW.1943-5460.0000082), 2011.

Johannessen, C.L., Davenport, W.A., Millet, A. and McWilliams, S.: The vegetation of the Willamette valley I. *Annals of the Association of American Geographers*, 61(2), pp-286-302, 1971.

Johnson S.L. and Jones J.A.: Stream temperature response to forest harvest and debris flows in western Cascades, Oregon. *Canadian Journal of Fisheries and Aquatic Sciences*, 57 (Suppl. 2), 30–39, doi.org/10.1139/cjfas-57-S2-30, 2000.

Kaushal, S. S., Likens, G. E., Jaworski, N. A., Pace, M. L., Sides, A. M., Seekell, D., Belt, D.H., Secor, R.L., and Wingate, R. L.: Rising stream and river temperatures in the United States. *Frontiers in Ecology and the Environment*, 8(9), 461-466, doi.org/10.1890/090037, 2010.

Kinouchi, T.: Impact of long-term water and energy consumption in Tokyo on wastewater effluent: implications for the thermal degradation of urban streams. *Hydrol. Process.* 21, 1207–1216. DOI: 10.1002/hyp.6680, 2007.

Knowles, N. and Cayan, D.: Potential Effects of Global Warming on the Sacramento/SanJoaquin Watershed and the San Francisco Estuary, *Geophys. Res. Lett.* 29, <https://doi.org/10.1029/2001GL014339>, 2002.

Landers D., Fernald A., Andrus C.: Off-channel Habitats. In: Willamette River Basin Planning Atlas (D. Hulse, S. Gregory and J. Baker, Eds.), pp. 26-27. Oregon State University Press, Corvallis, 2002.

Lee, K.: Stream Velocity and Dispersion Characteristics Determined by Dye-Tracer Studies on Selected Stream Reaches in the Willamette River Basin, Oregon. U.S. Geological Survey Water-Resources Investigations Report 95–4078, 1995.

Liang, S., Wang, W., Zhang, D., Li, Y., & Wang, G.: Quantifying the impacts of climate change and human activities on runoff variation: case study of the upstream of Minjiang River, China. *Journal of Hydrologic Engineering*, 25(9), 05020025, 2020.

Mantua, N., Tohver, I., and Hamlet, A.: Climate change impacts on streamflow extremes and summertime stream temperature and their possible consequences for freshwater salmon habitat in Washington State. *Climatic Change*, 102(1), 187-223, <https://doi.org/10.1007/s10584-010-9845-2>, 2010.

Markovic, D., Scharfenberger, U., Schmutz, S., Pletterbauer, F., and Wolter, C.: Variability and alterations of ~~water temperature~~water temperatures across the Elbe and Danube River Basins. *Climatic Change* 119, -375–389, doi.org/10.1007/s10584-013-0725-4, 2013.

Mayer, T.D.: Controls of summer stream temperature in the Pacific Northwest. *Journal of Hydrology*, 475, 323-335. <https://doi.org/10.1016/j.jhydrol.2012.10.012>, 2012.

Monthly Weather Review (MWR): American Meteorological Society, Online ISSN: 1520-0493, Volume 9 to 17, 1881-1889.

Moore, A. M.: Correlation and analysis of ~~water temperature~~water temperature data for Oregon Streams. United States Geological Survey Water-Supply Paper 1818-K, 53 pages, 1967.

Moore, A. M.: ~~Water temperature~~Water temperatures in the lower Columbia River. United States Geological Survey, Circular 551, doi.org/10.3133, 1968.

Formatted: Font color: Auto

1593 Mote, P.W.: Trends in temperature and precipitation in the Pacific Northwest during the twentieth century. Washington State University, 2003.

1594 Mote, P.W., Parson E. A., Hamlet, A. F., Keeton, W. S., Lettenmaier D., Mantua, N, Miles, E.

1595 L., Peterson, D. W., Peterson, D. L., Slaughter, R., and Snover, A.K.: Preparing for Climatic Change: The Water, Salmon, and Forests of the Pacific Northwest. Climatic

1596 Change 61, no. 1-2, 45-88, doi.org/10.1023/A:1026302914358, 2003.

1597 Mote, P. W., and Salathé, E. P.: Future climate in the Pacific Northwest. Climatic

1598 change, 102(1), 29-50, doi.org/10.1007/s10584-010-9848-z, 2010.

1600 Mote, P.W., Rupp, D.E., Li, S., Sharp, D.J., Otto, F., Uhe, P.F., Xiao, M., Lettenmaier, D.P.,

1601 Cullen, H. and Allen, M. R.: Perspectives on the cause of exceptionally low 2015 snow-

1602 pack in the western United States, Geophysical Research Letters, 43,

1603 doi:10.1002/2016GLO69665, 2016.

1604 Mote, P. W., Li, S., Lettenmaier, D. P., Xiao, M., and Engel, R.: Dramatic declines in snowpack

1605 in the western US. Npj Climate and Atmospheric Science, doi:10.1038/s41612-018-0012-

1606 1, 2018.

1607 Mote, P.W., Abatzoglou, J., Dello, K.D., Hegewisch, K., and Rupp, D.E.: Fourth Oregon Cli-

1608 mate Assessment Report. Oregon Climate Change Research Institute. occri.net/ocar4; ac-

1609 cessed online February 4, 2019, 2019.

1610 Naik, P. K. and D. A. Jay.: Human and climate impacts on Columbia River hydrology and salm-

1611 onids. River Research and Applications, 27, 1270-1276, DOI:10.1002/rra.1422, 2011.

1612 National Research Council.: Managing the Columbia River: Instream Flows, Water Withdraw-

1613 als, and Salmon Survival, Washington, DC: The National Academy Press.

1614 <https://doi.org/10.17226/10962>, 2004.

1615

1616 National Academies of Sciences, Engineering, and Medicine 2022. An Approach for Assessing

1617 U.S. Gulf Coast Ecosystem Restoration: A Gulf Research Program Environmental Moni-

1618 toring Report. Washington, DC: The National Academies Press.

1619 <https://doi.org/10.17226/26335>

1620 Nelson, K. C., & Palmer, M. A.: Stream temperature surges under urbanization and climate

1621 change: data, models, and responses, JAWRA journal of the American water resources

1622 association, 43(2), 440-452, <https://doi.org/10.1111/j.1752-1688.2007.00034.x>, 2007.

1623 Notch, J.J., McHuron, A.S., Michel, C.J., Cordoleani, F., Johnson M., Henderson, M.J. and Am-

1624 mann, A.J.: Outmigration survival of wild Chinook salmon smolts through the Sacra-

1625 mento River during historic drought and high water conditions. Environ Biol

1626 Fish 103, 561–576. <https://doi.org/10.1007/s10641-020-00952-1>, 2020.

1627 Olden J. D. and R. J. Naiman.: Incorporating thermal regimes into environmental flows assess-

1628 ments: modifying dam operations to restore freshwater ecosystem integrity. Freshwater

1629 Biology, 55, 86–107, doi.org/10.1111/j.1365-2427.2009.02179.x, 2010.

1630 Oregon Department of Environmental Quality (OR-DEQ): Willamette Basin TMDL and

1631 WQMP. Chapter 4: Temperature-Mainstem TDML and subbasin Summary. Accessed

1632 from <https://www.oregon.gov/deq/wq/tmdls/Pages/willamette2006.aspx>, accessed 2021-

1633 08-21, 2006.

1634 Palmer, M. A., Lettenmaier, D. P., Poff, N. L., Postel, S. L., Richter, B., & Warner, R.: Climate

1635 change and river ecosystems: protection and adaptation options, Environmental manage-

1636 ment, 44, 1053-1068, <https://doi.org/10.1007/s00267-009-9329-1>, 2009.

1637

Formatted: Font: (Default) Times New Roman, 12 pt

Formatted: Indent: Left: 0", Hanging: 0.5", Space After: 6 pt, Line spacing: single

Formatted: Font: (Default) Times New Roman, 12 pt

Formatted: Font: (Default) Times New Roman, 12 pt

Formatted: Font: (Default) Times New Roman, 12 pt

Formatted: Font: (Default) Times New Roman, 12 pt

Formatted: Font: (Default) Times New Roman, 12 pt, Not Italic

Formatted: Font: (Default) Times New Roman, 12 pt

Formatted: Font: (Default) Times New Roman, 12 pt, Not Italic

Formatted: Font: (Default) Times New Roman, 12 pt

Formatted: Font: 16 pt

Formatted: Font: Not Italic

Formatted: Font: Not Bold

Formatted: Font: (Default) Times New Roman, 12 pt

Formatted: Font: (Default) Times New Roman, 12 pt

Formatted: Font: (Default) Times New Roman, 12 pt

Formatted: Font: (Default) Times New Roman, 12 pt, Not Italic

Formatted: Font: (Default) Times New Roman, 12 pt

Formatted: Font: (Default) Times New Roman, 12 pt, Not Italic

Formatted: Font: (Default) Times New Roman, 12 pt

Formatted: Font: (Default) Times New Roman, 12 pt

Formatted: Font: 16 pt

Payne, S. K.: Dams. In: Willamette River Basin Planning Atlas (D. Hulse, S. Gregory and J. Baker, Eds.), pp. 30-31. Oregon State University Press, Corvallis, 2002.

Petersen, J. and Kitchell, J.: Climate regimes and ~~water temperature~~~~water temperature~~ changes in the Columbia River: Bioenergetic implications for predators of juvenile salmon. ~~Canadian Journal of Fisheries and Aquatic Sciences.~~ ~~CAN J FISHERIES AQUAT SCI.~~ 58: 1831-1841. 10.1139/cjfas-58-9-1831, 2001.

Piegay, H., Bornette G., Citterio A., Herouin, E., Moulin, B., and Statiotis, C.: Channel instability as a control on silting dynamics and vegetation patterns within perifulvial aquatic zones. Hydrological Processes 14: 3011-3029, 2000.

Peipoch, M., Brauns, M., Hauer, F.R., Weitere, M. and Valett, H.M.: Ecological simplification: human influences on riverscape complexity. BioScience, 65(11), pp.1057-1065, 2015.

Pohle I., Helliwell, R., Aube, C., Gibbs, S., Spencer, M. and Spezia, L.: Citizen science evidence from the past century shows that Scottish rivers are warming. Sci. Tot. Envr. 10.1016/j.scitotenv.2018.12.325, 2019.

Ralston, D.K., Talke, S.A., Geyer, W. R., Al'Zubadaei H., and Sommerfield, C. K.: Bigger tides, less flooding: Effects of dredging on water level in the Hudson River estuary. Journal of Geophysical Research, 124(1), doi: 10.1029/2018JC014313, 2019.

Richter, A. and Kolmes, S.A.: Maximum temperature limits for Chinook, coho, and chum salmon, and steelhead trout in the Pacific Northwest. Reviews in Fisheries Science 13:23-49, DOI: 10.1080/10641260590885861, 2005.

Rounds, S.A.: Thermal effects of dams in the Willamette River basin, Oregon: U.S. Geological Survey Scientific Investigations Report 2010-5153, 64 p, 2010.

Rounds, S.A.: Temperature effects of point sources, riparian shading, and dam operations on the Willamette River, Oregon: U.S. Geological Survey Scientific Investigations Report 2007-5185, 34 p. (Also available at <http://pubs.usgs.gov/sir/2007/5185/>), 2007.

Sedell, J.R. and Froggatt, J.L.: Importance of streamside forests to large rivers: The isolation of the Willamette River, Oregon, USA, from its floodplain by snagging and streamside forest removal, Internationale Veriningung fur Theoretische und Angewandte Limnologie Verhandlungen (International Association for Theoretical and Applied Limnology) 22, 1828-1834, 1984.

Steel, E. A., and Lange, I. A.: Using wavelet analysis to detect changes in water temperaturewater temperature regimes at multiple scales: Effects of multi-purpose dams in the Willamette River basin. River Research and Applications, 23(4), 351-359, doi.org/10.1002/rra.985, 2007.

Steel, E. A., Tillotson, A., Larsen, D. A., Fullerton, A. H., Denton, K. P., & Beckman, B. R.: Beyond the mean: the role of variability in predicting ecological effects of stream temperature on salmon. Ecosphere, 3(11), 1-11, doi.org/10.1890/ES12-00255.1, 2012.

Scott, M.H.: Statistical Modeling of Historical Daily ~~water temperature~~~~Water Temperatures~~ in the Lower Columbia River. Master of Sciences Thesis, Civil and Environmental Engineering, Portland State University, Portland, OR, USA, 2020. <https://doi.org/10.15760/etd.7466>

Scott, M.H., Talke, S.A., Jay, D.A. and Diefenderfer, H.: Warming of the Columbia River, 1853 to 2018. ~~Submitted to Accepted in River Research and Applications, Water Resources Research, Submission 2022WR033330, 20222023 (In Press).~~

Formatted: Font: (Default) Times New Roman, 12 pt

Formatted: Font: (Default) Times New Roman, 12 pt

Formatted: Indent: Left: 0", Hanging: 0.5", Space After: 6 pt, Line spacing: single

Formatted: Font: (Default) Times New Roman, 14 pt

Formatted: Font: 16 pt

Formatted: Font: (Default) Times New Roman, 12 pt

Formatted: Font: (Default) Times New Roman, 12 pt, Not Bold

Formatted: Font: (Default) Times New Roman, 12 pt

Formatted: Font: (Default) Times New Roman, 12 pt

Formatted: Font: (Default) Times New Roman, 12 pt, Not Italic

Formatted: Font: (Default) Times New Roman, 12 pt

Formatted: Font: (Default) Times New Roman, 12 pt

Formatted: Font: (Default) Times New Roman, 12 pt

1683 Sedell, J.R. and Froggatt, J.L.: Importance of streamside forests to large rivers: The isolation of
 1684 the Willamette River, Oregon, USA, from its floodplain by snagging and streamside for-
 1685 est removal, Internationale Veriningung fur Theoretische und Angewandte Limnologie
 1686 Verhandlungen (International Association for Theoretical and Applied Limnology) 22,
 1687 1828–1834, 1984.

1688 Steel, E. A., and Lange, I. A.: Using wavelet analysis to detect changes in water temperature re-
 1689 gimes at multiple scales: Effects of multi-purpose dams in the Willamette River basin,
 1690 River Research and Applications, 23(4), 351-359, doi.org/10.1002/rra.985, 2007.

1691 Steel, E. A., Tillotson, A., Larsen, D. A., Fullerton, A. H., Denton, K. P., & Beckman, B. R.: Be-
 1692 yond the mean: the role of variability in predicting ecological effects of stream tempera-
 1693 ture on salmon, Ecosphere, 3(11), 1-11, doi.org/10.1890/ES12-00255.1, 2012.

1694 Swain, S. S., Mishra, A., Chatterjee, C., & Sahoo, B.: Climate-changed versus land-use altered
 1695 streamflow: A relative contribution assessment using three complementary approaches at
 1696 a decadal time-spell, Journal of Hydrology, 596, https://doi.org/10.1016/j.jhy-
 1697 drol.2021.126064, 2021.

1698 Talke, S.A., Mahedy, A., Jay, D.A., Lau, P., Hilley, C., and Hudson, A.: Sea level, tidal and river
 1699 flow trends in the Lower Columbia River Estuary, 1853-present, Journal of Geophysical
 1700 Research-Oceans. <https://doi.org/10.1029/2019JC015656>, 2020.

1701 Taylor, J.E.: Making Salmon: An Environmental History of the Northwest Fisheries Crisis.
 1702 University of Washington Press, 488pp, 1999.

1703 Thilenius, J.F., 1968. The Quercus garryana forests of the Willamette valley, Oregon. Ecology,
 1704 49(6), pp.1124-1133.

1705 Thompson, P. R., Widlansky, M. J., Hamlington, B. D., Merrifield, M. A., Marra, J. J., Mitchum,
 1706 G. T., and Sweet, W.: Rapid increases and extreme months in projections of United
 1707 States high tide flooding. Nature Climate Change, 11(7), 584-590,
 1708 doi.org/10.1038/s41558-021-01077-8, 2021.

1709 Toffolon, M. and Piccolroaz, S.: A hybrid
 1710 model for river water temperature, water temperature as a function of air temperature and
 1711 discharge, Environ. Res. Lett., 10, 114011, https://doi.org/10.1088/1748-
 1712 9326/10/11/114011, 2015.

1712 U.S. Census: Statistics of The United States (Including Mortality, Property, &c.,) in 1860; com-
 1713 plied from the original returns and being the final exhibit of the Eighth Census. Depart-
 1714 ment of the Interior, Washington D.C., Government Printing Office, 1866.

1715 USC&GS (US Coast and Geodetic Survey): Surface water temperature ~~Water Temperature~~ and
 1716 Density, Pacific Coast North and South America & Pacific Ocean Islands. U.S. Govern-
 1717 ment Printing Office, Rockville, Maryland, 1967.

1718 USGS (United States Geological Survey): Willamette River Bathymetric Survey —
 1719 Willamette River water temperature ~~Water Temperature~~ Investigation. Retrieved July 28,
 1720 2022. https://or.water.usgs.gov/projs_dir/will_tmdl/main_stem_bth.html, 2003.

1721 Voelkel J. , Hellman D., Sakuma R., and Shandas V.: Assessing Vulnerability to Urban Heat: A
 1722 Study of Disproportionate Heat Exposure and Access to Refuge by Socio-Demographic
 1723 Status in Portland, Oregon, —International Journal of Environmental Research and Public
 1724 Health, DOI: 10.3390/ijerph15040640, 2018.

1725 Vose, R.S., Easterling, D.R., Kunkel, K.E., LeGrande, A.N. & Wehner, M.F.: Temperature
 1726 changes in the United States. In: Climate Science Special Report: Fourth National Cli-
 1727 mate Assessment, Volume I [Wuebbles, D.J., D.W. Fahey, K.A. Hibbard, D.J. Dokken,

Formatted: Font color: Auto

Formatted: Font color: Auto

Formatted: Font color: Auto

Formatted: Highlight

Formatted: Font: (Default) Times New Roman, 12 pt

Formatted: Font: (Default) Times New Roman, 12 pt

Formatted: Font: 14 pt

Formatted: Font: (Default) Times New Roman, 12 pt

1728 B.C. Stewart, and T.K. Maycock (eds.)]. U.S. Global Change Research Program, Wash-
 1729 ington, DC, USA, pp. 185-206, doi: 10.7930/JON29V45, 2017,
 1730 Waananen, A. O., Harris, D. D., & Williams, R. C. (1970). *Floods of December 1964 and*
 1731 *January 1965 in the Far Western States; Part 1 Description and Part 2 Stream flow and*
 1732 *sediment data* (US Geological Survey Water Supply Papers 1866A&B), Washington, D.C.
 1733
 1734 Wagner, R. W, Stacey, M.T., Brown, L.R. and Dettinger. M.: Statistical models of temperature
 1735 in the Sacramento-San Joaquin delta under climate-change scenarios and ecological im-
 1736 plications, *Estuaries and Coasts*, 34: 544-556, [https://doi.org/10.1007/s12237-010-](https://doi.org/10.1007/s12237-010-9369-z)
 1737 9369-z, 2011.
 1738 Wallick, J.R., Grant, G., Lancaster, S., Bolte, J.P. and Denlinger, R.: Patterns and controls on
 1739 historical channel change in the Willamette River, Oregon USA. *Large Rivers: Geomor-*
 1740 *phology and Management*, Second Edition, pp.737-775, 2022.
 1741 Webb B.W. and Walling D.E.: Temporal variability in the impact of river regulation on thermal
 1742 regime and some biological implications, *Freshwater Biology*, 29, 167–182,
 1743 doi.org/10.1111/j.1365-2427.1993.tb00752.x 1993.
 1744 Webb, B. W., Clack, P.D., and Walling, D.E.: Water-air temperature relationships in a Devon
 1745 river system and the role of flow, *Hydrological Processes*, 17, 3069-3084,
 1746 <https://doi.org/10.1002/hyp.1280>, 2003.
 1747 Webb, B. W. and Nobilis, F.: Long-term changes in river temperature and the influence of cli-
 1748 matic and hydrological factors, *Hydrological Sciences Journal*, 52(1): 74-85,
 1749 doi.org/10.1623/hysj.52.1.74, 2007.
 1750 Weber, C., Nilsson, C., Lind, L., Alfredsen, K. T., and Polvi, L. E.: Winter disturbances and riv-
 1751 erine fish in temperate and cold regions, *BioScience*, 63(3), 199-210,
 1752 doi.org/10.1525/bio.2013.63.3.8, 2013.
 1753 White, S.M., Justice, C. Kelsey, D.A., McCullough, D.A. and Smith, T.: Legacies of stream
 1754 channel modification revealed using General land Office surveys, with implications for
 1755 ~~water temperature~~ *water temperature* and aquatic life, *Elementals: Science of the An-*
 1756 *thropocene* 5(3). <https://doi.org/10.1525/elementa.192>, 2017.
 1757 White, R.H., Anderson, S., Booth, J.F. et al.: The unprecedented Pacific Northwest heatwave of
 1758 June 2021. *Nat Commun*, 14, 727, <https://doi.org/10.1038/s41467-023-36289-3>, 2023.
 1759 Willingham, W.F.: *Army Engineers and the Development of Oregon*. United States Army Corps
 1760 of Engineers, Portland, 259 pp, 1983.
 1761 Zhu, S, Nyarko, E.K., and Hadzima-Nyarko, M.: Modelling daily ~~water temperature~~ *water tem-*
 1762 *perature* from air temperature for the Missouri River. *PeerJ*,
 1763 <https://doi.org/10.7717/peerj.4894>, 2018 Jun 7;6:e4894. doi: 10.7717/peerj.4894, 2018.

Formatted: Font: 14 pt

Formatted: Font: (Default) Times New Roman

Formatted: Font: (Default) Times New Roman

Formatted: Font: (Default) Times New Roman, Italic

Formatted: Font: Italic

Formatted: Font: (Default) Times New Roman

Formatted: Font: (Default) Times New Roman

Formatted: Font: (Default) Times New Roman

Formatted: Font: (Default) Times New Roman

Formatted: Font: (Default) Times New Roman

Formatted: Font: (Default) Times New Roman

Formatted: Font: (Default) Times New Roman

Formatted: Font: (Default) Times New Roman, 12 pt

Formatted: Font: (Default) Times New Roman, 12 pt

Formatted: Font: (Default) Times New Roman, 12 pt, Not Bold

Formatted: Font: (Default) Times New Roman, 12 pt

Formatted: Font: (Default) Times New Roman, 12 pt

Formatted: Font: (Default) Times New Roman, 12 pt